2D nanostructures: Potential in diagnosis and treatment of Alzheimer's disease

Saba Tufail [a,*], Mohammad Asif Sherwani [b], Zahid Shamim [c], Abdullah [d], Khang Wen Goh [e], Mohammad N. Alomary [f], Mohammad Azam Ansari [g], Abdulaziz Abdullah Almosa [h], Long Chiau Ming [i,*], Amar Daud Iskandar Abdullah [j,*], Farheen Badrealam Khan [k,l,**], Asma Al Menhali [k,*], Sameer Mirza [m,*], Mohammed Akli Ayoub [l,*]

[a] Department of Genetics, University of Alabama at Birmingham, Birmingham, AL, USA
[b] Department of Dermatology, University of Alabama at Birmingham, Birmingham, AL, USA
[c] Department of Electrical Engineering, Faculty of Engineering and Technology, Aligarh Muslim University, Aligarh, India
[d] Department of Pharmacy, University of Malakand, Khyber Pakhtunkhwa, Pakistan
[e] Faculty Data Science and Information Technology, INTI International University, Nilai, Malaysia
[f] Advanced Diagnostic and Therapeutic Institute, King Abdulaziz City for Science and Technology, Riyadh, Saudi Arabia
[g] Department of Epidemic Disease Research, Institute for Research and Medical Consultations (IRMC), Imam Abdulrahman Bin Faisal University, Dammam, Saudi Arabia
[h] Wellness and Preventive Medicine Institute, King AbdulAziz City of Science and Technology, Riyadh, Saudi Arabia
[i] Department of Medical Sciences, School of Medical and Life Sciences, Sunway University, Sunway City, Malaysia
[j] Department of Biological Sciences, School of Medical and Life Sciences, Sunway University, Sunway City, Malaysia
[k] Department of Biology, College of Science, United Arab Emirates University, Al Ain, United Arab Emirates
[l] Department of Biological Sciences, College of Medicine and Health Sciences, Khalifa University, PO Box 127788, Abu Dhabi, United Arab Emirates
[m] Department of Chemistry, College of Science, United Arab Emirates University, Al Ain, United Arab Emirates

A B S T R A C T

Two-dimensional (2D) nanomaterials have garnered enormous attention seemingly due to their unusual architecture and properties. Graphene and graphene oxide based 2D nanomaterials remained the most sought after for several years but the quest to design superior 2D nanomaterials which can find wider application gave rise to development of non-graphene 2D materials as well. Consequently, in addition to graphene based 2D nanomaterials, 2D nanostructures designed using macromolecules (such as DNAs, proteins, peptides and peptoids), transition metal dichalcogenides, transition-metal carbides and/or nitrides (MXene), black phosphorous, chitosan, hexagonal boron nitrides, and graphitic carbon nitride, and covalent organic frameworks have been developed. Interestingly, these 2D nanomaterials have found applications in diagnosis and treatment of various diseases including Alzheimer's disease (AD). Although AD is one of the most debilitating neurodegenerative conditions across the globe; unfortunately, there remains a paucity of effective diagnostic and/or therapeutic intervention for it till date. In this scenario, nanomaterial-based biosensors, or therapeutics especially 2D nanostructures are emerging to be promising in this regard. This review summarizes the diagnostic and therapeutic platforms developed for AD using 2D nanostructures. Collectively, it is worth mentioning that these 2D nanomaterials would seemingly provide an alternative and intriguing platform for biomedical interventions.

1. Introduction

Over the years, it has been envisaged that the distinctive architecture and properties of two-dimensional (2D) nanomaterials have made them the focal point of research amongst scientific community across the globe [1–8]. The development of graphene 2D materials brought such a

turning point in the area of materials science that its discoverers were awarded the Noble Prize. Numerous structurally related 2D nanomaterials, such as transition metal dichalcogenide nanosheets and 2D polymers have since appeared [7,9]. Interestingly, scientists have succeeded in assembling functional 2D nanomaterials from macromolecular assemblies such as DNAs, proteins, peptides and peptoids (or poly-N-substituted glycine) with well-orchestrated structural skeletons and a high degree of information encoded by side-chain residue sequences [7,10–17]. Due to their benefits in realizing tailor-made and sequence-specific properties, such type of 2D nanomaterials have garnered increasing interest.

Alzheimer's disease (AD) is a distressing neurodegenerative (ND) condition and a leading contributor of dementia in the elderly population worldwide [18–21]. Of note, progressive nerve cell degeneration is the hallmark of AD, resulting in deterioration of cognitive functions. As a matter of fact, the brain areas viz. the hippocampus and cerebral cortex, which are directly linked to memory functioning and higher intellectual, unfortunately there is reduced cholinergic transmission in AD condition [22]. β-amyloid (Aβ) aggregates have been shown by a large body of research to form the basis of AD-associated senile (amyloid) plaques, contributing to neuronal death and cognitive dysfunction. Of note, it is

envisaged that more than 82 million people would be affected by this untreatable disease by 2030 and this figure is expected to rise in near future, as per recent reports [23]. To tackle this growing epidemic, early diagnosis and prompt care are incredibly needed. To this end, various techniques for the diagnosis and treatment of AD have been explored, one of which is nanostructure exploitation. Interestingly, the use of nanoparticles (nps) for diagnostic and therapeutic applications against AD is associated with vast evidence. However, in the design of therapeutics and diagnostics against AD; 2D nanostructures, while superior to nps in general, have only lately gained recognition. It is reasonable to argue that owing to free obverse and reverse surfaces, 2D nanostructures have a wide surface area and are thus seemingly superior in taking a sizeable amount of payload to different locations. In addition, free obverse and reverse surfaces in 2D nanostructures often make it possible for more than one drug to be loaded concurrently, making them suitable for hybrid therapies as well.

Considering these aspects, it is reasonable to argue that with ever-increasing demand in healthcare sector for novel, efficient, and rapid technologies for the diagnosis and therapeutic of AD, together with the fact that 2D nanostructures provides vast scope for evolution of newer generation of biomedical applications. Herein, we discuss various 2D
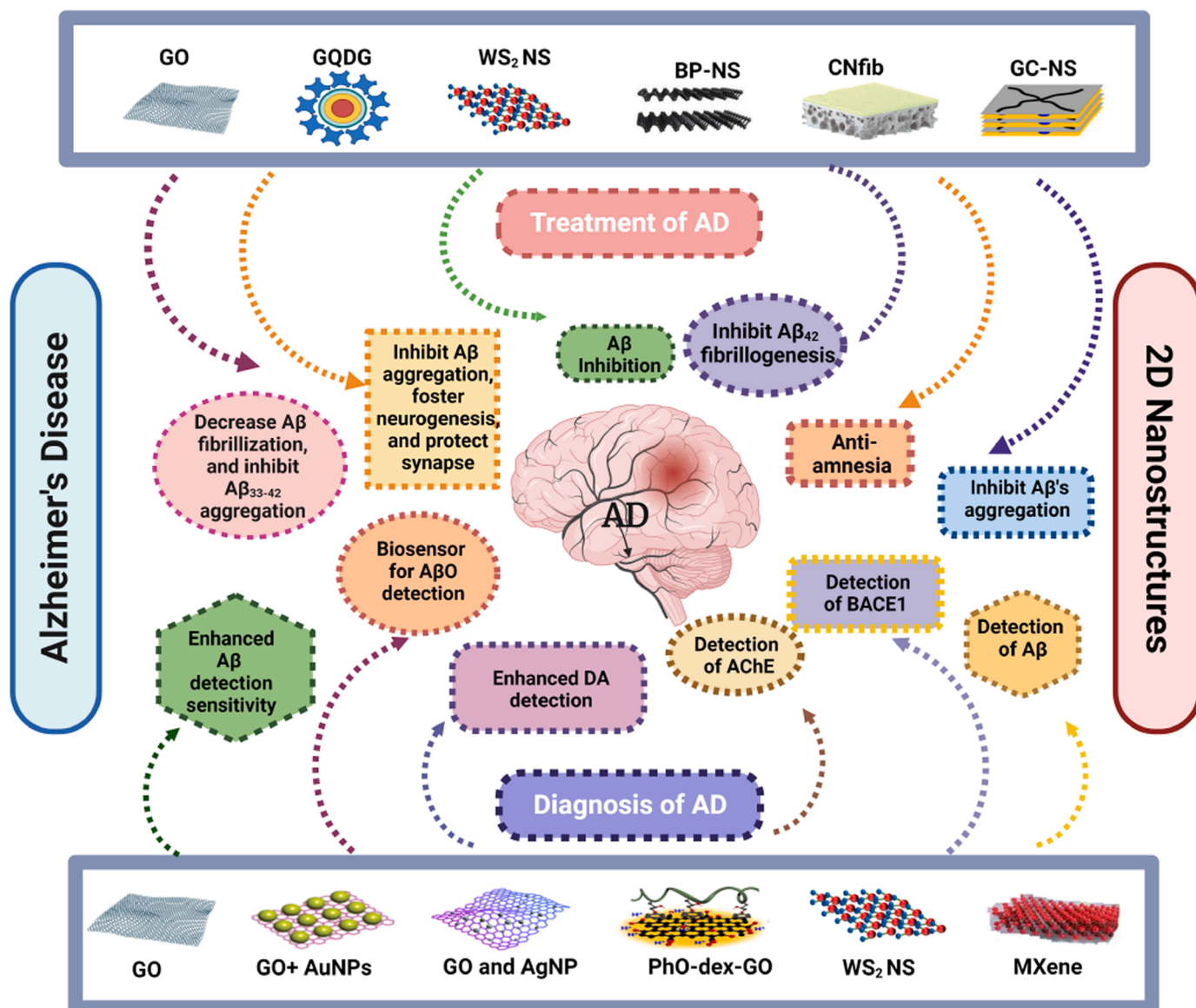

Fig. 1. Representative figure highlighting various 2D nanomaterials for therapeutic intervention of AD.

nanostructures that have been documented to date in the diagnosis and/ or treatment of AD. Fig. 1 represents the various 2D nanomaterials employed in diagnosis and treatment of AD (Fig. 1); whereas Table 1 highlights the different 2D nanomaterials in diagnosis and treatment of AD (Table 1). Interestingly, as more and more are gleaned about their intricacies; they will be highly instrumental in revolutionizing the field of biomedical applications against disease which have long been acknowledged as untreatable.

2. 2D nanostructures in diagnosis of Alzheimer's disease

On a global scale, AD is increasingly being realised as one of the most important medical and social problems of elderly population and it is projected to double every 20 years as the population ages [24]. Despite extensive research on AD, there is neither confirmed pathological clarity of AD nor effective therapy available as of now. Although the precipitation of Aβ peptide that results in the formation of β-amyloid plaques, and intracellular tau protein aggregation forming neurofibrillary tangles, are the main biomarkers that appear in cerebrospinal fluid (CSF) and blood several years before the appearance of symptoms. It has always been emphasized that to prevent the disease, early diagnosis is absolutely needed [25]. In 2018, the National Institute on Aging-Alzheimer's Association declared quantitative estimation of AD biomarkers in CSF as diagnostic criterion for AD condition [25–27]. Nonetheless, the invasiveness and pain caused by taking fluid from CSF via lumbar puncture, has limited its public applicability. Over the years, it has been envisaged that these biomarkers from CSF leaks into the blood stream owing to breaching of the blood brain barrier (BBB) caused by AD condition [28–31]. Accordingly, these biomarkers can be detected in the blood samples by non-invasive and sensitive method [32]. In the journey of advancing the current conventional AD diagnostic tools from post-symptomatic to the pre-symptomatic stage, there is a dire need for the development of novel diagnostic tools that are reliable, cost-effective, highly accurate, and non-invasive [33].

In this connection, 2D nanostructures-impregnated biosensors are gaining popularity due to their exceptional physicochemical properties, high specificity, ultra-sensitivity, low cost and user friendliness [34,35]. Based on the applied transducer technology, the biosensors can be basically classified into optical [36], piezoelectric [37], and electrochemical biosensors [38] and so on. Optical biosensors are subdivided into fluorescent, colorimetric, and luminescent biosensors. Fluorescent and luminescent biosensors are enzymes or florescent dyes-based biosensors [39–41]. 2D nanomaterials such as transition metal dichalcogenides and black phosphorus (BP) are basically applied in optical biosensors [42–44]. Of note, the fluorescent biosensors, the most commonly used optical biosensors, employ fluorescent detectors for the detection of the ligand. 2D nanomaterials viz. Molybdenum disulfide nanosheets-based fluorescent (MoS2 NSs) biosensor was used for the detection of Aβ oligomers [45]. Similarly, graphene-oxide (GO) was been employed for the detection of tau proteins [46], and WS2 nanosheets had been utilized for detection of miR-29a in human serum samples [47]. Further, piezoelectric biosensors basically can detect antigens (Ags) in solid and liquid states as a function of change in the mass of substrate. Interestingly, it can detect the analytes (Ags) in the picogram range based on change in frequency occurring as a result of receptor-antigen interaction. Additionally, this biosensor can be applied for detection of viruses, DNA hybridization, detection of cancer etc [48]. Moreover, electrochemical biosensors represent another most commonly used system, as they offer several advantages including low cost, portability, high sensitivity, user friendliness, determination of analyte in turbid samples, and compatibility thereof [49,50]. Further, electrochemical biosensors convert biochemical signals to amperometric signal, wherein electrons are either created or used. Thereafter, the respective transducers (conductometric, potentiometric, or impedimetric) generate the signal [51,52]. Examples of electrochemical biosensors are amperometric, potentiometric, and conductometric

Table 1
Representative table highlighting various 2D nanostructures in diagnosis and treatment of AD.

S. No.	Type of nanostructures	Examples	Mechanism	References
Diagnosis of AD				
	Graphene based nanostructures	Graphene oxide (GO)	Adsorption/ desorption of Aβ and enhance sensitivity	[22]
		Reduced GO	Enhances electrochemical activity as biosensor for DNA	[59,60]
		GO+ AuNPs	Biosensor to track amyloid-beta oligomers (AβO)	[64]
		GO	Biosensor for detection of miRNA-34a	[59,65, 68]
		GO and Ag-NP	Enhanced detection of DA	[69,70]
		Phenoxy-modified dextran-GO (PhO-dex-GO)	Detection of AChE	[184]
		Au electrode deposited with rGO sheets and AuNPs	Improved DA detection	[72]
		Dual-layered rGO	Determination of Aβ$_{1-42}$ in plasma	[62]
		Au/NiFe2O4 @GO-Ch	Detection of Aβ$_{1-42}$	[23]
		GO-AgNPs-CS-PSS-CS	Detection of Aβ$_{1-42}$	[77]
		GO@LbL-AuNPs	Detection of Tau-441	[78]
	Peptoid nanosheets	Antibody-mimetic peptoid nanosheets	Detection of Aβ42	[20,58]
	Transition metal dichalcogenides	WS$_2$ nanosheets	Detection of miR-29a and Aβ	[85]
		WS$_2$ nanosheets-based florescence sensor	Detection of β-secretase (BACE1)	[105]
	MXene 2D nanomaterials	MXene (d-Ti3C2TxMXene) and (MWCNTs)-based sensor	Detection of Aβ	[111]
Treatment of AD				
	Graphene based nanostructures	GO	Slow down Aβ fibrillization, inhibit aggregation of Aβ$_{33-42}$	[127,130]
		Thioflavin-modified GO + NIR laser irradiation	Dissociation of amyloid deposits	[135]
		Graphene quantum dots (GQDG)	Inhibit aggregation of Aβ (1-42), foster neurogenesis, and protect synapse	[137]
		GO with protein-coated GO	Inhibition of Aβ fibrillation via adsorption of Aβ monomers	[128]
		GO plus carbon nanodots, and nanotubes	Significant inhibition of Aβ$_{33-42}$ aggregation	[131,132]
	WS$_2$ nanosheets	WS$_2$	Aβ inhibition	[141]
	Black phosphorus nanosheets (BP-NS)	BP Nanosheets	Antioxidant effect by decreasing ROS induced cytotoxicity	[142]
		PEG-LK7 @BP	Inhibit Aβ$_{42}$ fibrillogenesis	[147]
		TiL$_4$ @BPNSs	Inhibit Aβ$_{40}$ via adsorption	[148]

(continued on next page)

Table 1 (*continued*)

S. No.	Type of nanostructures	Examples	Mechanism	References
	Chitosan (CS) based drug nanofilm	CNfib	Reduces amnesia	[149]
	Graphitic carbon nitride nanosheets	g-C3N4 nanosheets	Inhibit Aβ's aggregation induced by metals, attenuates neurotoxicity, decreases intracellular ROS	[152]
		g-C3N4 @Pt	Inhibit Aβ fibrillation	[152]
		g-C3N4/GO	Aβ fibrils disaggregation	[164]
	Molybdenum disulfide-quantum dots	Triphenyl-phosphonium bromide-molybdenum disulfide-quantum dots (TPP-MoS2 QDs)	Decreased Aβ-mediated neurotoxicity, eliminated Aβ aggregates, prevent neuro-inflammation, and M1/M2 microglial polarization	[165]
	Hexagonal boron nitride (h-BN)	hBN- NPs	Attenuated Aβ-induced neurotoxicity via decreasing necrosis and apoptosis, suppressed EGFR and TNF-α and activated BDNF.	[176]
	Covalent organic frameworks (COFs)	2D COFs	Aβ aggregation inhibition	[180]
	MXene	Nb2C nanosheets	Chelate transition metal ions and alleviate oxidative stress	[181]

biosensors [53,54]. 2D nanomaterials such as GO has been used in electrochemical detectors for the detection of Aβ42 [55]. Moreover, screen printed electrode (SPE) impregnated reduced GO-gold (Au) nanowire nanocomposite has been applied for the detection of miRNA-137, one of the biomarkers of AD [56]. Similarly, reduced graphene oxide {(rGO)-AuNPs} has been employed in electrochemical biosensors for the detection of Tau-441 [57].

In summation, it has always been emphasized that early diagnosis of AD is pre-requisite. Nevertheless, current diagnostic methods using CSF and imaging biomarkers are extremely costly and invasive as already mentioned [58]. To this end, interestingly but not surprisingly, 2D nanostructures represents prospective diagnostic agents for AD and many labs have reported promising results as detailed below.

2.1. Graphene based nanostructures in diagnosis of AD

Graphene and graphene derivatives are the most widely exploited nanomaterials in developing immunosensors for AD. Basically, it is a 2D nanosheet of carbon atoms and finds wide applications due to its various intriguing properties including large surface area, ease of functionalization, high tensile strength, and good thermal and electrical conductivity. In fact, one of the most sought-after applications of graphene is biosensor development [59].

GO, a graphene derivative, is a 2D single atomic layer of carbon atoms arranged in a honeycomb lattice. It is a water-soluble graphene derivative and is basically obtained by functionalizing graphene with oxygen containing groups. This functionalization facilitates the adsorption and desorption of molecules for improving sensitivity.

Further, reduced GO (rGO), another derivatized GO, was first documented in electrochemical biosensors as an electrode modifier by Zhou and group for DNA sensing [59,60] showing improved electrochemical activity in comparison to graphite electrodes. Since then, various types of biosensors, including AD biosensors, have integrated graphene and its derivatives.

Interestingly, various accumulating evidence have highlighted the potential of various GO dependent nanostructures for the diagnosis of AD. It has been found that through π-π interactions and other interactions, GO can adsorb Aβ monomers. Interestingly, graphene biosensors can detect incredibly low concentrations of biomarkers [22] and plausibly this is because the presence or lack of a few analyte molecules will produce a detectable difference in the electrical properties of graphene [61]. For the determination of beta-amyloid (Aβ$_{1-42}$) in plasma, a research group delineated a label-free platform based on dual-layered graphene and rGO. [62] Interestingly, a limit of detection (LOD) of 2.398 pM over a wide linear range from 11 pM to 55 nM, was achieved for Aβ$_{1-42}$ biomarkers [24]. Further, a dual detection system to detect serum miR-137, Azimzadeh *et al.*, have delineated a high-sensitivity electrochemical biosensor with Au nanowires (AuNWs) and rGO. Intriguingly, their findings showed a linear spectrum of 5.0 to 750.0 fM for identification with an LOD of 1.7 fM. Interestingly, this platform has been able to distinguish non-specific analytes from the target analytes and displayed strong identification in actual serum samples [56].

As a matter of fact, amyloid-beta oligomers (AβO) represent one of the signature biomarkers related to AD [63,64]. To this end, Sun et al. [65] developed gold NPs (AuNPs) and GO based electrochemical hydrogel biosensors to track AβO. Interestingly, AuNPs and GO were highly sensitive and selective for AβO and do not bind Aβ-monomers or fibrils. Intriguingly, the soft graphene hydrogel electrode facilitates quick movement of biomolecules into the electrode owing to high surface area. Moreover, the shape and volume of hydrogel electrode can be altered to adjust its conductivity [66]. Likewise, AuNPs have unique plasmonic band, high extinction coefficient, and can be functionalized with several biomolecules [67]. Basically, for the development of AβO sensor platform, the cellular prion protein (PrPC) peptide was adsorbed on to the built electrode. The intricate relation on the hydrogel electrode between PrPC probes and AβO improved the electron transfer resistance. For the detection of AβO, the biosensor displayed high precision. AβO can be preferentially distinguished from amyloid beta (Aβ) fibrils or monomers. In addition, in artificial CSF or blood plasma, detection of AβO (up to 0.1 pM) was highly sensitive. Interestingly but not surprisingly, for AβO detection, the linear range from 0.1 pM - 10 nM was achieved [65].

Further, another study employed GO as an electrode modifier for the development of a RNA sensor platform especially for detection of miRNA-34a, an AD biomarker. [68] Firstly, they allowed reaction of electrochemically triggered pencil graphite electrodes with ethyl-carbodiimide hydrochloride/ N-hydroxysuccinimide (EDC/NHS) and thereafter with GO to increase the electrode surface area and facilitate miRNA immobilization, producing single GO sensors for use [59,68]. This solution offered an economical and user-friendly sensor system that allows fewer chemical reagents to be used, both of which are essential attributes for the device's transferability. The miRNA-34a concentration was calculated on phosphate buffer saline (PBS) by electrochemical impedance spectroscopy (EIS), exhibiting LOD of 261.7 nM thereof.

As a matter of fact, neurotransmitters which are the endogenous chemicals that enable communication among neurons, facilitate synaptic and cognitive activity. It has been envisaged that the neurological diseases (ND) such as AD have been attributed to small fluctuations in neurotransmitters synthesis or release, so they have been suggested to be appropriate biomarkers for the diagnosis and treatment of ND disorders. Toyos-Rodríguez et al., and Shin et al. [59,69] recommended a biosensor for the identification of dopamine (DA) for AD. They obtained a lower LOD relative to preceding investigations that used Au or carbon-based nanomaterials by employing an indium tin oxide (ITO) working

electrode modified with GO and silver nps, enhancing biosensing efficiency at low levels of DA [70,71]. The electrochemical detection of DA was achieved by direct detection by differential pulse voltammetry (DPV), cyclic voltammetry (CV), and amperometry of the oxidation phase of this molecule. Further, ascorbic acid (AA) and uric acid (UA) have been used for biosensor selectivity assessment because they have an oxidative propensity close to that of DA and other neurotransmitters and are found at higher concentrations in blood samples [72]. Of note, at 0.2 μM stages, the biosensor showed a particular reaction to DA.

Park et al. [73] have also detected DA with a Au electrode amended by a nanocomposite of rGO sheets and AuNPs. Because of their great conductivity, rGO sheets were utilized to increase the sensitivity of the biosensor, while AuNPs were integrated to improve electrocatalytic activity. Interestingly selectivity was accomplished as rGO sheet electrons appear to form bonds with benzene rings of the molecules like DA. Nonetheless, other interfering entities with a structure analogy to DA, such as AA, can however, influence the biosensor's selectivity. For this purpose, the assay was optimized at pH 7.4, wherein AA exists as an anion and DA exists as a cation, thereby promoting DA's electrostatic contact with the surface of the electrode. Interestingly but not surprisingly, DA was detected with a LOD of 0.098 μM at many fold higher interfering concentration of AA. In analogy, Lee et al. [74] built a biosensor using AuNPs and rGO as electrode modifiers to detect norepinephrine (NE). NE is a neurotransmitter with monoamine that is closely linked to neuronal disorders. The key downside of NE detection; however, is its resemblance to UA and AA, as they have comparable potential for electrochemical oxidation. Of note, NE detection with a LOD of 200 nM was achieved by this biosensor even in environment with many folds' higher concentration of the interfering agents.

Further, a platform for the discernment of H_2O_2 as a possible biomarker of oxidative stress (OS) was developed by Wang and group [75]. This platform was dependent on the usage of rGO functionalized glass carbon electrode (GCE) blended with electrodeposition-generated Au, Fe_3O_4 and platinum (Pt) nps. This electrode platform was placed in cell culture media for in vitro detection of H_2O_2 as it was released by cells under conditions of OS, triggered by the introduction of AA. Without the need for enzymatic labels, the changes in H_2O_2 was determined by CV, giving a LOD of 0.1 μM, which greatly decreased the study time. As a matter of fact, the identification of H_2O_2 is an important method of tracking OS, which is of particular significance today, especially in the study of AD. Albeit, further research into the intricacies of OS in AD clientele prior to the application of these platforms is in any case necessary.

It has been envisaged that the measurement of the conformation (monomer, oligomer, or fibril) of amyloid peptide aggregates would be seemingly instrumental in the therapeutic intervention for AD. To this end, systematic study of the amyloid conformation using analytical methods is also important for the accurate quantification of the relative quantities of the three amyloid peptide conformations. To this end, Jeong et al. [76] developed a multiplexing biosensor based on rGO that can be employed to track the relative quantities of the three different amyloid β-40 (Aβ-40) conformations. Interestingly, a multisensor capable of independently detecting the different conformations in a single fluid sample was reported. They demonstrated that their method showcased robust analytical sensitivity at 1 pg/mL and a relatively broad dynamic range spanning from 1 pg/mL to 10 ng/mL for each Aβ-40 conformation. Different amyloid solutions including monomeric Aβ-40, aggregated Aβ-40, and disaggregated Aβ-40 solutions were used to check if the rGO sensor system could be employed to determine the relative quantities of these conformations. Notably, in each amyloid solution, multiple patterns were found in the relative quantities of the three conformations, suggesting that these intricacies could act as a significant aspect in the clinics.

In addition, Devi et al. [23] developed an accurate and ultrasensitive electrochemical immunosensor based on a AuNPs/nickel ferrite-decorated GO-CS nanocomposite (Au/NiFe2O4 @GO-Ch) modified GCE for determination of amyloid beta peptide (βA$_{1-42}$) as an efficient sensing medium. The combinatorial amalgam of highly conductive NPs of Au and NiFe2O4 on 2D GO nanosheets offered an outstanding platform. They immobilized βA antibody (Ab) onto the surface of Au/NiFe2O4 @GO-Ch/GCE through carbodiimide chemistry and developed a compact Au/NiFe2O4 @GO-Ch/GCE immunosensor. Their findings indicated that the immunosensor selectively detected βA$_{1-42}$ and exhibited a broad linear detection range spanning 1 pg/mL to 1 ng mL^{-1}, with a LOD as low as 3.0 pg/mL. In addition, by detecting βA$_{1-42}$ in CSF, the immunosensor also demonstrated its clinical viability.

Further, Nagare and Patil [77] fabricated surface plasmon resonance (SPR) biosensor based on GO surface decorated chitosan (CS) for highly selective and sensitive detection of Aβ$_{1-42}$. In brief, they fabricated AgNPs and GO via green technology approach. Thereafter, polystyrene sulphonate (PSS) and CS were deposited on the surface of AgNPs (AgNPs-CS-PSS-CS) to design layer-by-layer (LbL) assembly followed by fixation of Aβ Abs onto the aforementioned structure resulting in an platform viz. AgNPs-CS-PSS-CS@anti-Aβ. Herein, it is pertinent to mention that CS provides amine functionality that offers numerous sites for coupling of anti-Aβ Abs. Interestingly but not surprisingly, the range of detection for Aβ$_{1-42}$ was 2 fg/mL to 400 ng/mL, while LOD was found to be 1.21 fg/mL.

In another study, Nagare and Patil [78] used GO based SPR biosensor for the identification of Tau-441. To this end, GO was fabricated by modified Hummer method, while the AuNPs were fabricated into LbL design via cationic and anionic polyelectrolytes (GO@LbL-AuN-Ps@Anti-Tau). Subsequently, immobilization of Anti-Tau rabbit Abs was carried out using carbodiimide chemistry. Intriguingly, LOD for Tau-441was found to be 13.25 fg/mL, while the range of detection was observed in the range from 150 ng/mL to 5 fg/mL.

Further, Murillo et al., used SiO2 NPs to gauge the Tau protein in serum samples using Interferometric Optical Detection Method (IODM) integrated with an Fabry–Perot Interferometers (FIP) biotransducer [79]. Interestingly, LOD for Tau protein was 10 pg/mL with a detection range of 1×10^{-2} ng/mL to 1×10^5 ng/mL.

2.2. Peptoid nanosheet in diagnosis of AD

It is envisaged that for the fabrication of 2D nanomaterials, sequence-defined macromolecules including DNAs, peptides, proteins, and peptoids have been employed recently as specific building blocks [7, 58,80,81]. These types of 2D nanomaterials offer the prospects of high selectivity and simple surface tunability owing to the sequence-specific molecular recognition inherent to these functional constituents. In addition, due to the huge disparities in the physical and chemical attributes of their parental constituents, they show distinct characteristics. Especially important amongst these sequence-defined 2D nanomaterials are those fabricated from peptoids since they are highly stable and immensely tunable.

Of note, 2D peptoid-assembled nanomaterials are a category of newly formed 2D material that has unique and attractive characteristics. Peptoids are synthetic sequence-defined molecules that resemble both peptides and proteins in their structure and function and amalgamate the properties of synthetic polymers and bio-polymers [82,83]. Interestingly, they can be synthesized cheaply and conveniently and have great variety in side-chains. In addition, peptoids are bio-compatible and demonstrate great potential for molecular recognition like proteins. Furthermore, they have high thermal and chemical stability, unlike peptides and proteins, and deliver the special simplicity of self-assembly and tuning functions since they lack inter- and intra-molecular hydrogen backbone bonds [84,85]. Therefore, the structures obtained from peptoids are easily synthesized and exhibit greater chemical and thermal stability compared to other forms of sequence-defined 2D nano-materials, and their surface chemistry and internal core can be more readily customized by altering the chemistry of peptoid side chains [1, 14]. These properties of peptoid-assembled nanomaterials make them a

suitable candidate for development of biosensor.

Interestingly, several reports suggest peptoid-based biosensors can be promising in designing AD diagnostics. To this end, Zhu *et al.* developed Ab mimetic self-assembling peptoid nanosheet for label-free serum-based diagnosis of AD [58]. The Ab mimetic peptoid nanosheets were functionalized with $A\beta_{42}$ recognizing surface exposed ADP3 loops. Interestingly, the loops owing to their high affinity for serum $A\beta_{42}$ were capable of detecting AD sera with high sensitivity. The peptoid nanosystem offered a scaffold, wherein the loops act as recognition probes by mimicking the architecture of Abs eliminating non-specific binding. Intriguingly, this 2D Ab-mimetic platform has shown great promise for blood-based diagnosis of AD and also opens avenues for designing alternative engineering of Abs and sensor development.

Further, Gao et al. [20] also exploited peptoid nanosheets fitted with $A\beta_{42}$ recognizing loops (ADP3) for developing a label-free assay using the high-throughput SPR imaging (SPRi) system. The loops were autonomously organized, resulting in the formation of peptoid nanosystem featuring surface exposed functional ADP3 loops. This nanosheet based biosensor system, in addition to carrying $A\beta_{42}$ recognizing loops, was linked to high throughput SPRi system for detecting plasma and sera of amnestic mild cognitive impairment (aMCI) and AD patients. Interestingly, this nanosheet-based sensor system has been shown to effectively differentiate samples from normal group and AD and amnestic MCI clienteles. This differentiation precedes the diagnostic success achieved using the $A\beta_{42}$-recognizing molecule and the $A\beta_{42}$-specific Ab, attributed to the analysis of varying amounts of $A\beta_{42}$ through SPRi. Therefore, it is justifiable to assert that this study provided early diagnosis of AD with a label-free, economical, exceptionally sensitive, and efficient blood-based test.

2.3. WS₂ nanosheet in diagnosis of AD

Transition metal dichalcogenides (TMDs) are an evolving group of layered nanomaterials that are highly dependent on structure and dimension in terms of their physicochemical properties [47,86–88]. By downsizing the number of layers to monolayers, the characteristics behaviours of the TMDs can be modulated, which makes them intriguing nanomaterials for use in different fields of study [89–94]. Interestingly, owing to their large surface areas, high surface reactivity, and solid Raman scattering signals, thin TMD nano-system have been employed as diagnostic and therapeutic materials for biological and medical applications [95–99]. As a matter of fact, WS₂ has been extensively used as a sensing material in fluorescent, electrochemical, photoelectrochemical, and SPR sensing platforms for the identification of molecules, metal ions and contaminants [47,100–105]. To detect DNA, microRNA, nuclease, and DNA glycosylases, biosensors focused on the interaction between single-stranded DNA (ssDNA) and WS₂ nanosheet have been manufactured [80,106–110]. In particular, in the forster resonance energy transfer (FRET)-based assays, TMD nanosheets, like WS₂, have shown high potential as a fluorescence quencher enabling rapid, swift, and specific detection of oligonucleotides [47]. Interestingly, the weak vander waals forces adsorb a dye-labelled ss DNA, contributing to fluorescence quenching, whilst a double-stranded DNA (dsDNA) is more likely to detach from the TMD nanosheets surfaces, that eventually causes the quenched fluorescence being restored.

Further, Kim et al. [47] reported modulation of WS₂ nanosheet interface by liquid-phase exfoliation and non-covalent functionalization with four different dextran polymers for the fluorescence-based determination of miR-29a, the microRNAs corresponding to the toxic Aβ peptides formation. Using the various interfaces of the WS2 nanosheets, the adsorption kinetics of a fluorescein labelled ssDNA (FAM-DNA) probe and the desorption kinetics of the FAM-DNA duplex with a target miR-29a were thereafter studied. The modulation of WS₂ interface produced alterations in thermodynamics attributes of the FAM-DNA probe. Of note, the WS₂ nanosheet-dependent FRET system was developed to specifically gauge the miR-29a; interestingly, this was achieved

by leveraging insights into the effects of device engineering processes.

As a matter of fact, β-secretase (BACE1) is an important drug target for AD therapy. To this end, Zuo et al. [80] delineated a simple and sensitive fluorescence biosensing system using WS₂ nanosheets for BACE1 detection. With a detection limit of 66 pM for BACE1, the proposed WS₂ nanosheet-based platform demonstrated superior specificity and high sensitivity. This biosensing platform can also be used for drug screening; and could be readily expanded by adjusting the peptide substrate sequence to identify various other proteases, including the detection of protease inhibitors. since the WS₂ nanosheet will serve as a common energy acceptor for various types of fluorescent dyes.

2.4. MXene 2D nanomaterial in diagnosis of AD

MXene is a 2D material composed of early transition metal carbides, carbonitrides and nitrides fabricated through the processing of elements from the MAX phases (M = Ti, V, Nb; A = the IIA and IVA elements; X = N and/or C). These systems are simple to produce and possess strong electrical, optical, mechanical and plasmonic properties [59, 111]. Interestingly, Ozcan et al. designed an intriguing platform for the identification of Aβ protein employing a mixture of delaminated titanium carbamide MXene (d-Ti3C2TxMXene) and multi-walled carbon nanotubes (MWCNTs) composite with polymers [112]. Basically, D-Ti3C2TxMXene was paired with MWCNTs in order to quench MXene from being aggregated. Finally, Aβ protein was imprinted on this platform and successfully utilized for the detection of the Aβ proteins in the biological fluid. Interestingly, these MXene 2D nanomaterials are increasingly explored for biosensor applications.

In summation, all these studies have highlighted the prospective potentials of 2D nanomaterials in the diagnosis of AD. However, it is also equally important that even though 2D nanostructures-based biosensors offer various advantages. Nevertheless, there are several challenges still exist that halt further development of biosensors and their application on large scale.

3. 2D nanostructures in treatment of Alzheimer's disease

As a matter of fact, protein aggregation has gained considerable interest in recent decades, owing to its strong correlation with several ND disorders including AD, Huntington's, and Parkinson's diseases [113–115]. Of note, amyloid fibrils, which represent the ultimate outcome of protein aggregation, exhibit a core structure characterized by cross-β configuration, featuring both vertical and inter-strand hydrogen bonds formed by β-strands aligned in parallel with the fibril axis [116]. Basically, after fibril nucleus formation, it rapidly grows into insoluble fibrils. The most cytotoxic species is commonly thought to be the β-sheet-rich oligomer [117,118]. There are no appropriate medications for the cure of AD so far. In order to identify successful therapeutic methods, researchers have made considerable strides to explore protein aggregation process. Different therapeutic methods have been put out and carried out so far to research the integration or disassembly of amyloid aggregates by regulating their molecular configurations and bonding interactions. Experimental studies have shown that nps including carbon nps, Au nps and polymer nps, small molecules, Abs, and proteins/peptides can prevent Aβ aggregation and/or target/dissociate Aβ aggregates [113,119–127]. Recently, 2D nanomaterials have garnered increasing attention as possible AD therapeutic because they have been found to either target the Aβ aggregation process, inhibit the synthesis of toxic oligomers and/or disrupt the amyloid fibrils. In the following sections, we have provided a glimpse of various 2D nanomaterials in the treatment of AD.

3.1. Graphene based nanostructures in treatment of AD

Graphene oxide (GO) has drawn considerable interest due to its good biocompatibility, high solubility and dispersibility, and low cytotoxicity

as discussed in the aforementioned sections [113]. There have been several laboratories that have shown that graphene and its derivatives have displayed tremendous prospects for the therapeutic intervention of AD, considering the above-mentioned excellent properties of graphene. For instance, Mahmoudi et al. [128] highlighted that the Aβ fibrillization process can be slowed by GO and protein-coated GO. Of note, the wide surface area of GO sheets was shown to block the process of Aβ fibrillation through amyloid monomer adsorption. Moreover, Yang et al. [129] found that not only GO suppress $A\beta_{1-40}$ fibrillization, but also effectively eliminates the advanced amyloid fibrils. Furthermore, Li and group highlighted that GO would interact with the aggregation mechanism of the $A\beta_{33-42}$, leading to considerably small fibrils in the presence of GO relative to long and intricately intertwined fibrils in the control. [130] Their additional research [131] found that GO shows a significant attenuation effect on the aggregation of $A\beta_{33-42}$. Further, they envisaged the impact of various shapes of carbon nps and GO on the aggregation of $A\beta_{33-42}$ [132] and found that GO nanosheets, accompanied by nanotubes and nanodots, had the greatest inhibitory effect. Additionally, another study showed that GO can not only effectively attenuate the aggregation of $A\beta_{1-42}$, but also reduces the toxicity issues of Aβ [133]. Interestingly, this experimental evidence GO exerts a substantial inhibitory impact on the aggregation of both $A\beta_{33-42}$ fragments and the full-length Aβ protein. Computationalists are increasingly focusing on the physical connections between GO and Aβ, inspired by these experimental works. Interestingly, Baweja et al. [134] used brief time-scale MD simulations to explore the influence of GO on the alpha-helix of the $A\beta_{1-40}$ monomer. Interestingly, their calculations revealed that the alpha-helix structure can partly be unfolded by GO. Additionally, another report stated that pristine graphenes seemingly interrupt the protofibrils of $A\beta_{16-22}$ [129]. They reported that GO can break mature amyloid fibrils into pieces and clear them off. Nevertheless, the underlying mechanism that underscores GO mediated inhibition of Aβ fibrillization; however, still remains incompletely understood.

Chen et al. [113] explored the association of GO on the accumulation of four $A\beta_{33-42}$ peptide in an attempt to elucidate the mechanism underlying the inhibition of Aβ aggregation by GO. They explored $A\beta_{33-42}$ oligomerization through molecular dynamics (MD) simulations of replica exchange on four $A\beta_{33-42}$ peptides, in the presence and absence of two separate GO sizes. Their simulations showed that isolated $A\beta_{33-42}$ can form expanded β-sheets and barrel-like structures of fibril; nonetheless, it was suppressed with GO nanosheets. They showed that GO seemingly prevents $A\beta_{33-42}$ oligomerization by having $A\beta_{33-42}$ peptides isolated from each other. GO_{120} showed a greater inhibitory effect with the same carbon atoms and oxidation groups than GO_{60} by having a greater effective touch surface area. Collectively, this research seemingly sheds light on the underlying molecular intricacies associated with GO's mediated attenuation of the aggregation of $A\beta_{33-42}$.

In addition, Li et al. [135] used GO for photothermal treatment of AD. High optical absorption of graphene within the near infrared region (NIR) region makes it a suitable candidate for photothermal therapy. Li *et al.* observed that amyloid deposits can be effectively dissociated using thioflavin-modified GO with NIR laser irradiation. However, the intricate dynamic process and the underlying molecular mechanisms responsible for the disassociation and elimination of pre-formed Aβ aggregates induced by graphene could not be fully elucidated.

Qing et al. [136] and Zhang et al. [137] used Cys enantiomorph-modified GO to inhibit $A\beta_{1-40}$ fiber elongation, nucleation, and adsorption processes. Interestingly, they reported that R-cysteine modulation in addition to preventing the development of amyloid fibril, also significantly influenced the transition of $A\beta_{1-40}$ from alpha-helix to β-sheet conformation. GO sheets were able to considerably slow and suppress the amyloid β fibrillation phase by adsorbing amyloid monomers. Moreover, another group engineered a novel platform by conjugating neuroprotective peptide with graphene quantum dots (GQDG). [138] Interestingly, they reported that GQDG was capable of inhibiting the aggregation of Aβ (1−42), protecting the synapse and

fostering neurogenesis, thereby contributing to improving the capacity for learning and memory. Further, Nedumpully-Govindan et al. [139] used discrete MD simulations to research the relationship between aggregates of human islet amyloid polypeptide (hIAPP) and GO. Their findings revealed that GO was able to prevent hIAPP aggregation. Hydrogen bonds and aromatic stacking have also been shown to drive the potential binding of hIAPP to GO nanosheets; and peptide-GO binding realistically blocked hIAPP's self-association and aggregation on the nanosheet surface [140].

Moreover, Zhang et al. [137] studied the intricacies of mature Aβ amyloid fibrils and graphene sheets by atomistic simulation. They showed that interaction of GO sheets with amyloid fibrils caused secondary structure damage in them seemingly because of adsorption of these fibrils onto GO nanosheets. Self-association and aggregation of amyloid fibrils was inhibited upon interaction with GO sheets because the hydrophobic interactions like van der Waals forces which are used for fibril self-aggregation start to be exploited for adsorption of fibrils on graphene sheets instead. Graphene nanosheets were found to effectively decompose preformed amyloid aggregates. Interestingly, their study provides structural analysis to better understand the mechanism of association between graphene and protein aggregates and may help devise superior nanotherapeutics for AD.

3.2. WS_2 nanosheet in treatment of AD

As discussed earlier, amyloid-β peptide (Aβ) polymerization into amyloid fibrils is a crucial stage in AD pathogenesis. Aβ aggregation inhibition and Aβ preformed fibril destabilization have promising results against AD and have been used in clinical trials. In order to efficiently prevent Aβ aggregation and dissociation of preformed Aβ aggregates using NIR irradiation, Li et al. [141] have shown the application of WS_2 nanosheets. WS_2 nanosheets are biocompatible and are superior to most previously documented Aβ inhibitors owing to their potential to breach the BBB. Van der Waals forces and electrostatic interactions facilitate adsorption of Aβ40 on WS2 nanosheets, preventing Aβ40 aggregation process. WS_2's peculiar strong NIR absorption property allows the breakdown of amyloid aggregates upon NIR irradiation. The hyperthermic effects of WS_2 nanosheets are important and beneficial in biological applications and development of multifunctional nanomaterials for the treatment of AD.

3.3. Black phosphorus nanosheets in treatment of AD

Being 2D semiconductor nanostructure analogue, black phosphorous (BP) is useful in numerous fields, including biomedicine, catalysis, optoelectronics, and energetics [142,143]. BP nanosheets are composed of phosphorous atoms which being negatively charged have high affinity towards metal ions [144–146]. Therefore, BP nanosheets also have high binding capacity for metal ions and hence act as efficient nanocaptor for them. Moreover, BP nanosheets also exhibit excellent photothermal and hyperthermic effect under NIR radiation. Considering these properties of BP nanosheets, Chen *et al.* [142] designed a neuroprotective nanomedicine against neurological disorders including AD using BP nanosheets. They found that among the typical metal ions (such as Ca^{2+}, Mg^{2+}, Fe^{2+}, Fe^{3+}, and Zn^{2+}) present in humans, BP nanosheets selectively bind to Cu^{2+}. BP nanosheets also serve as an antioxidant to decrease the cytotoxic reactive oxygen species (ROS) generation associated with Cu^{2+} dyshomeostasis. BP suffers from some drawbacks including low functionality, and quick degradation that have been reduced by Yang et al., [147] via coupling of an Aβ inhibitor (LK7) and stabilization with PEG (PEG-LK7 @BP). These nanosheets exhibited augmented Aβ inhibition that could reduce the manifestations of AD. Similarly, Lim et al., [148] prepared titanium ligand modified BP (TiL4 @BP) nanosheets that inhibited the formation of $A\beta_{40}$ fibrils via adsorption of Aβ40 monomers. The TiL4 @BP prevented the elongation of fibrils that contributed to the attenuation of AD.

Chen *et al.* give evidence by in vitro and in vivo experiments that permeability of BP nanosheets to cross BBB is enhanced through the photothermal effect, which makes them superior to other drug molecules, small chemicals or peptides that are unable to cross the BBB. The increased permeability of BP nanosheets improves the drug efficacy. Moreover, the high durability and exceptional biocompatibility of BP nanosheets provide ND therapy with outstanding biosafety. These intriguing functions make BP nanosheets a potential therapeutic choice for ND to control Cu^{2+} concentrations and reduce symptoms associated with oxidative stress.

3.4. Chitosan based nanofilm in treatment of AD

CS is a natural substance and exists as a non-branched unit containing glucose polysaccharide. CS is extensively explored in drug delivery models because of its superior biodegradability, biocompatibility, and low immunogenicity actions. The antimicrobial action of chitin and CS against species such as bacteria, yeasts and fungi has been observed [149,150]. It has been envisaged that the polycationic and electrostatic stacking design of CS facilitates its interaction with the bacterial cell and results in its bio-efficacy. For efficient oral drug delivery, various PEG stabilized multifactorial systems of CS with other molecular assembles have been reported [149]. Further, various nanostructures have been designed using CS, including nps, nanofibres and nanofilms with varied functionalities. CS nps have been used for various drug delivery purposes; nevertheless, recently, various other functions of CS nanofibers and nanofilms have being increasingly explored. CS nanofibers have many benefits including high porosity and a high volume-to-surface ratio that increases the loading potential for the easy loading of drugs into nanofibers. Generally, thin films are capable of increasing the initiation of drug action, reducing the frequency of doses, and enhancing medication effectiveness. Thin films are also effective in removing the drug's side effects and reducing the substantial proteolytic enzyme-induced degradation. Therefore, scientific fraternity is inclined to develop CS thin films and exploit it for various biomedical uses. Development of drug-loaded CS thin films have been reported and demonstrated mucoadhesive property that facilitated release of the drug within the buccal mucosa [151]. The promising results of CS nanofilms have persuaded scientists to examine it in various other diseases including AD. To this end, Reddy et al. [149] has developed CS nanofilms, loaded with donepezil drug and evaluated their potential for treatment of AD. Interestingly, CS nanofilms released donepezil in a sustained manner and thereby exhibited prospective potential to become a therapeutic for AD.

3.5. Graphitic carbon nitride nanosheet in treatment of AD

Graphitic carbon nitride (g-C_3N_4) is the most stable carbon nitride allotrope under atmospheric conditions and owing to its intriguing semiconductor properties, has drawn considerable interest [152–161]. Recently, in bioimaging applications, 2D ultra-thin g-C_3N_4 nanosheets with a higher surface area-to-volume ratio have been used as fluorosensors due to their strong fluorescence, intriguing biocompatibility, and non-toxic properties [162,163].

The surface functionalities of g-C_3N_4, i.e. NH_2/-NH-/=N-, have recently been shown to be well-characterized ligands displaying high adsorption potential for metal ions [152,153]. An interesting platform consisting of platinum(II)- g-C_3N_4 nanosheet (g-C3N4 @Pt) was developed by Li and group [153]. This system potentially binds Aβ and thereby interfere with their aggregation process and thus attenuates the toxicity issues of the peptide aggregates. Additionally, they found that g-C_3N_4 @Pt nanosheets have strong photocatalytic properties and can oxygenate Aβ with visible light irradiation, which greatly attenuates both Aβ's aggregation strength and eventually neurotoxicity thereof.

Li et al. [153] further reported that the g-C_3N_4 nanosheet can serve as a nanochelator to considerably attenuate the Aβ aggregation and

disintegrate the preformed Aβ–Cu^{2+} aggregates. In clinical trials for AD treatment, metal-ion chelation therapy has been employed. In this context, g-C_3N_4 nanosheets employed as Aβ inhibitors for AD treatment, demonstrating the capability to coordinate Cu^{2+} ions. Interestingly, the g-C_3N_4 nanosheets can considerably attenuate the production of Aβ aggregates, disintegrate the preformed Aβ-Cu^{2+} aggregates, minimize oxidative stress and shield the cells from the toxicities associated with Aβ.

Further, as a matter of fact, protein misfolding leads to the formation of fibrils, oligomers, and Aβ plaques that culminates in AD. Therefore, modulation of Aβ peptide aggregates could be a strategy for the treatment of AD. To this end, Wang et al., [164] fabricated g-C3N4/GO based 2D materials for the irreversible disaggregation of Aβ fibrils following UV irradiation. By using advanced analytical techniques, they found that g-C3N4/GO effectively resulted in disaggregation of $Aβ_{33–42}$.

3.6. Molybdenum disulfide-quantum dots treatment of AD

Several studies have focused on the treatment of AD by eliminating Aβ by nanoparticle affinity, however, instead of neurons the nanoparticles are taken by microglia, leading to poor AD control. In order to resolve the issue, Ren et al., [165] formulated nanozymes based on triphenyl-phosphonium bromide-molybdenum disulfide quantum dots (TPP-MoS2 QDs). These quantum dots after crossing the BBB, ameliorate neuroinflammation, escape the lysosomes, target mitochondria, and eliminate Aβ aggregates, thereby helping to alleviate AD.

3.7. Hexagonal boron nitride in treatment of AD

Boron nitride (BN) is a synthetic compound having layered lattice structure, good insulator, lubricant, resistant to oxidation and chemicals, and excellent thermoelectric properties [166–169]. BN has different crystal structure at different temperature and pressure including hexagonal, cubic, rhombic, and wurstitic. Among these, hexagonal boron nitride (h-BN) is the most stable form at room temperature [170,171]. It has been demonstrated that the h-BN NPs exert cytoprotective activity against $Aβ_{1–42}$ induced AD model by several mechanisms including attenuation of oxidative stress [172], reduction of necrosis/apoptosis [173,174] and anti-inflammatory effect [175]. Ayden *et al.,* studied the effects of various concentrations of h-BN against $Aβ_{1–42}$ induced neurotoxicity. They concluded that h-BN attenuates Aβ-induced neurotoxicity via decreasing necrosis and apoptosis, suppression of epidermal growth factor receptor (EGFR), Tumor necrosis factor alpha (TNF-α), and activated brain-derived neurotrophic factor (BDNF) [176].

3.8. Covalent organic frameworks (COFs) in treatment of AD

These are highly biocompatible newer generation nps containing carbon, nitrogen, and oxygen [177]. Being porous covalent organic materials, they find application for therapeutic intervention of AD [178, 179]. Owing to their highly tunable structure, the 2D-COFs can cross BBB and inhibit Aβ aggregation. Interestingly, it has been found via molecular modelling and simulation studies that 2D-COFs impregnated with amine moieties inhibits Aβ aggregation [180].

3.9. MXenes in treatment of AD

Transition metal dyshomeostasis is one of key factor for the aggregation of Aβ peptides. Excess transition metal ions (particularly Cu^{2+}) trigger oxidative stress, neuroinflammation, and apoptosis of neurons. Therefore, Du et al., designed a chelating agent based on 2D niobium carbide (Nb_2C) for the inhibition of Cu^{2+} induced oxidative stress, and AD [181]. Likewise, Jian *et al.,* devised vanadium carbide (V_2C) based 2D MXenes and demonstrated that these 2D MXenes inhibit 4-hydroxynonenal, an oxidative stress biomarker. In addition, they found the upregulation of tyrosine hydroxylase (TH), and the downregulation of

ionized calcium binding adapter molecule 1 (Iba-1) after administration of V$_2$C-based 2D MXenes, that resulted in the inhibition of neuro-inflammation, and improved synthesis of dopamine, thus helping to eliminate AD [182].

Collectively, all these studies have highlighted the prospective potentials of 2D nanomaterials in AD. There is great enthusiasm in the 2D nanomaterial research fraternity that these materials will certainly help in fight against various debilitating including AD. At this moment time, it is also equally important to argue that despite the extensive pre-clinical studies on 2D nanomaterials, there is still scarcity of clinical studies [183]. It is envisaged that the 2D platforms discussed in this review may offer a blueprint for the creation of new multifactorial nanomaterials employed for the therapeutic intervention of AD.

4. Conclusions

The prevalence of AD is rising every day and the social and economic burden associated with this debilitating condition is increasing. Early diagnosis and timely therapeutic intervention are of utmost importance. 2D nanomaterials have been examined as possible diagnostic and therapeutic platforms. Albeit, accumulating evidence demonstrate that these 2D nanomaterials are intriguing contenders for emerging biomedical applications. Nonetheless, still there remains many challenges to be addressed to pave their way to clinical trials; as more and more is gleaned about their intricacies; they will be highly instrumental in revolutionizing the field of biomedical applications against disease which have long been recognised as untreatable. In fact, the pursuit of fascinating studies like those mentioned above are crucial in the realm of early diagnosis for this debilitating and incurable disorder.

Abbreviations

AA, Ascorbic acid; Aβ, β-amyloid; AβO, amyloid-beta oligomers; AChE, acetylcholinesterase; AD, Alzheimer's disease; ADI, Alzheimer's Disease International; Ag-NP, silver nanoparticles; AuNPs, gold nanoparticles; aMCI, amnestic mild cognitive impairment; AuNWs, gold nanowires; BACE1, β-secretase 1; BBB, blood brain barrier; BDNF, brain-derived neurotrophic factor; BP, black phosphorus; BP-NS, black phosphorus nanosheets; CEA, carcinoembryonic antigen; COFs, covalent organic frameworks; CS, chitosan; CSF, cerebrospinal fluid; CV, cyclic voltammetry; DA, dopamine; DPV, differential pulse voltammetry; dsDNA, double-stranded DNA; EDC, ethylcarbodiimide hydrochloride; EGFR, epidermal growth factor receptor; EIS, electrochemical impedance spectroscopy; FAM-DNA, fluorescein labelled ssDNA; fg, femtogram; fM, femtomole; FRET, Forster resonance energy transfer; GCE, glass carbon electrode; g-C3N4, graphitic carbon nitride; GO, graphene oxide; h-BN, hexagonal boron nitride; ITO, indium tin oxide; LbL, layer-by-layer; LOD, limit of detection; MoS2, molybdenum disulfide nanosheets; MXene, transition-metal carbides and/or nitrides; Nb2C, niobium carbide; ND, neurological disorders; ng, nanogram; NE, norepinephrine; NHS, N-hydroxysuccinimide; NIR, near-infra red; NSs, nanosheets; PBS, phosphate buffer saline; PEG, polyethylene glycol; pg, picogram; PhO-dex, phenoxy-modified dextran; PrPC, thiolated cellular prion protein; PSS, polystyrene sulphonate; Pt, platinum; rGO, reduced graphene oxide; SPE, screen printed electrode; SPR, surface plasmon resonance; ssDNA, single-stranded DNA; ThT, Thioflavin T; TMDs, transition metal dichalcogenides; TNF-α, Tumor necrosis factor alpha; TPP-MoS2 QDs, Triphenyl-phosphonium bromide-molybdenum disulfide-quantum dots; UA, uric acid; WHO, World Health Organization; WS$_2$, Tungsten disulfide.

CRediT authorship contribution statement

Conceptualization: S.T., M.A.S., F.B.K., L.C.M. Software: S.T., M.A.S., F.B.K., K.W.G. Resources: F.B.K., Z.S., K.W.G., L.C.M. Writing—original draft preparation: S.T., M.A.S., F.B.K., Z.S., A., Writing—review and editing: M.A.A., K.W.G., L.C.M., A.A.A., A.A.M., A.D.I.A. Visualization: S.T., M.A.S., F.B.K., K.W.G. Supervision: S.T., F.B.K., A.D.I.A., S.M., M.N. A. Project administration: S.T., M.A.S., F.B.K., A.A.M.

Declaration of Competing Interest

There are none

Data Availability

No data was used for the research described in the article.

References

[1] E.J. Robertson, A. Battigelli, C. Proulx, R.V. Mannige, T.K. Haxton, L. Yun, S. Whitelam, R.N. Zuckermann, Design, synthesis, assembly, and engineering of peptoid nanosheets, Acc. Chem. Res. 49 (3) (2016) 379–389.

[2] C. Tan, H. Zhang, Two-dimensional transition metal dichalcogenide nanosheet-based composites, Chem. Soc. Rev. 44 (9) (2015) 2713–2731.

[3] Y. Guo, K. Xu, C. Wu, J. Zhao, Y. Xie, Surface chemical-modification for engineering the intrinsic physical properties of inorganic two-dimensional nanomaterials, Chem. Soc. Rev. 44 (3) (2015) 637–646.

[4] G.R. Bhimanapati, Z. Lin, V. Meunier, Y. Jung, J. Cha, S. Das, D. Xiao, Y. Son, M. S. Strano, V.R. Cooper, L. Liang, S.G. Louie, E. Ringe, W. Zhou, S.S. Kim, R. R. Naik, B.G. Sumpter, H. Terrones, F. Xia, Y. Wang, J. Zhu, D. Akinwande, N. Alem, J.A. Schuller, R.E. Schaak, M. Terrones, J.A. Robinson, Recent advances in two-dimensional materials beyond graphene, ACS nano 9 (12) (2015) 11509–11539.

[5] X. Sun, Z. Liu, K. Welsher, J.T. Robinson, A. Goodwin, S. Zaric, H. Dai, Nano-graphene oxide for cellular imaging and drug delivery, Nano Res. 1 (3) (2008) 203–212.

[6] A.K. Geim, K.S. Novoselov, The rise of graphene, Nat. Mater. 6 (3) (2007) 183–191.

[7] P. Mu, G. Zhou, C.-L. Chen, 2D nanomaterials assembled from sequence-defined molecules, Nano-Struct. Nano-Objects 15 (2018) 153–166.

[8] P. Ares, K.S. Novoselov, Recent advances in graphene and other 2D materials, Nano Mater. Sci. 4 (1) (2022) 3–9.

[9] L. Wang, Y. Li, L. Zhao, Z. Qi, J. Gou, S. Zhang, J.Z. Zhang, Recent advances in ultrathin two-dimensional materials and biomedical applications for reactive oxygen species generation and scavenging, Nanoscale 12 (38) (2020) 19516–19535.

[10] Y. Suzuki, G. Cardone, D. Restrepo, P.D. Zavattieri, T.S. Baker, F.A. Tezcan, Self-assembly of coherently dynamic, auxetic, two-dimensional protein crystals, Nature 533 (7603) (2016) 369–373.

[11] T. Jiang, C. Xu, Y. Liu, Z. Liu, J.S. Wall, X. Zuo, T. Lian, K. Salaita, C. Ni, D. Pochan, V.P. Conticello, Structurally defined nanoscale sheets from self-assembly of collagen-mimetic peptides, J. Am. Chem. Soc. 136 (11) (2014) 4300–4308.

[12] J.D. Brodin, X.I. Ambroggio, C. Tang, K.N. Parent, T.S. Baker, F.A. Tezcan, Metal-directed, chemically tunable assembly of one-, two- and three-dimensional crystalline protein arrays, Nat. Chem. 4 (5) (2012) 375–382.

[13] W. Liu, H. Zhong, R. Wang, N.C. Seeman, Crystalline two-dimensional DNA-origami arrays, Angew. Chem. Int Ed. Engl. 50 (1) (2011) 264–267.

[14] H. Jin, F. Jiao, M.D. Daily, Y. Chen, F. Yan, Y.H. Ding, X. Zhang, E.J. Robertson, M.D. Baer, C.L. Chen, Highly stable and self-repairing membrane-mimetic 2D nanomaterials assembled from lipid-like peptoids, Nat. Commun. 7 (2016), 12252.

[15] F. Jiao, Y. Chen, H. Jin, P. He, C.L. Chen, J.J. De Yoreo, Self-repair and patterning of 2D membrane-like peptoid materials, Adv. Funct. Mater. 26 (48) (2016) 8960–8967.

[16] P. Wang, S. Gaitanaros, S. Lee, M. Bathe, W.M. Shih, Y. Ke, Programming self-assembly of DNA origami honeycomb two-dimensional lattices and plasmonic metamaterials, J. Am. Chem. Soc. 138 (24) (2016) 7733–7740.

[17] Y. Suzuki, M. Endo, H. Sugiyama, Lipid-bilayer-assisted two-dimensional self-assembly of DNA origami nanostructures, Nat. Commun. 6 (2015), 8052.

[18] K. Blennow, M.J. de Leon, H. Zetterberg, Alzheimer's disease, Lancet 368 (9533) (2006) 387–403.

[19] J.L. Cummings, Alzheimer's disease, N. Engl. J. Med. 351 (1) (2004) 56–67.

[20] H. Gao, M. Liu, Z. Zhao, C. Yang, L. Zhu, Y. Cai, Y. Yang, Z. Hu, Diagnosis of mild cognitive impairment and Alzheimer's disease by the plasma and serum amyloid-beta 42 assay through highly sensitive peptoid nanosheet sensor, ACS Appl. Mater. Interfaces 12 (8) (2020) 9693–9700.

[21] D.S. Knopman, H. Amieva, R.C. Petersen, G. Chételat, D.M. Holtzman, B. T. Hyman, R.A. Nixon, D.T. Jones, Alzheimer disease, Nat. Rev. Dis. Prim. 7 (1) (2021) 33.

[22] M. Bilal, M. Barani, F. Sabir, A. Rahdar, G.Z. Kyzas, Nanomaterials for the treatment and diagnosis of Alzheimer's disease: an overview, NanoImpact 20 (2020), 100251.

[23] R. Devi, S. Gogoi, H.S. Dutta, M. Bordoloi, S.K. Sanghi, R. Khan, Au/NiFe(2)O(4) nanoparticle-decorated graphene oxide nanosheets for electrochemical immunosensing of amyloid beta peptide, Nanoscale Adv. 2 (1) (2020) 239–248.

[24] H.Y. Abbasi, Z. Tehrani, A. Devadoss, M.M. Ali, S. Moradi-Bachiller, D. Albani, O. J. Guy, Graphene based electrochemical immunosensor for the ultra-sensitive label free detection of Alzheimer's beta amyloid peptides Aβ(1-42), Nanoscale Adv. 3 (8) (2021) 2295–2304.

[25] P. Scheltens, K. Blennow, M.M. Breteler, B. de Strooper, G.B. Frisoni, S. Salloway, W.M. Van der Flier, Alzheimer's disease, Lancet 388 (10043) (2016) 505–517.

[26] P. Scheltens, B. De Strooper, M. Kivipelto, H. Holstege, G. Chételat, C. E. Teunissen, J. Cummings, W.M. van der Flier, Alzheimer's disease, Lancet 397 (10284) (2021) 1577–1590.

[27] RA. Ossenkoppele, C. Groot, R. Smith, O. Strandberg, S. Palmqvist, E. Stomrud, P. Tideman, T. Ohlsson, J. Jögi, et al., Amyloid-β and tau PET scans predict clinical progression in cognitively unimpaired people, Nat. Med. 28 (11) (2022) 2267–2268.

[28] S. Palmqvist, S. Janelidze, Y.T. Quiroz, H. Zetterberg, F. Lopera, E. Stomrud, Y. Su, Y. Chen, G.E. Serrano, A. Leuzy, N. Mattsson-Carlgren, O. Strandberg, R. Smith, A. Villegas, D. Sepulveda-Falla, X. Chai, N.K. Proctor, T.G. Beach, K. Blennow, J.L. Dage, E.M. Reiman, O. Hansson, Discriminative accuracy of plasma phospho-tau217 for Alzheimer disease vs other neurodegenerative disorders, Jama 324 (8) (2020) 772–781.

[29] A. Nakamura, N. Kaneko, V.L. Villemagne, T. Kato, J. Doecke, V. Doré, C. Fowler, Q.X. Li, R. Martins, C. Rowe, T. Tomita, K. Matsuzaki, K. Ishii, K. Ishii, Y. Arahata, S. Iwamoto, K. Ito, K. Tanaka, C.L. Masters, K. Yanagisawa, High performance plasma amyloid-β biomarkers for Alzheimer's disease, Nature 554 (7691) (2018) 249–254.

[30] S. Janelidze, N. Mattsson, S. Palmqvist, R. Smith, T.G. Beach, G.E. Serrano, X. Chai, N.K. Proctor, U. Eichenlaub, H. Zetterberg, K. Blennow, E.M. Reiman, E. Stomrud, J.L. Dage, O. Hansson, Plasma P-tau181 in Alzheimer's disease: relationship to other biomarkers, differential diagnosis, neuropathology and longitudinal progression to Alzheimer's dementia, Nat. Med. 26 (3) (2020) 379–386.

[31] E.H. Thijssen, R. La Joie, A. Strom, C. Fonseca, L. Iaccarino, A. Wolf, S. Spina, I. E. Allen, Y. Cobigo, H. Heuer, L. VandeVrede, N.K. Proctor, A.L. Lago, S. Baker, R. Sivasankaran, A. Kieloch, A. Kinhikar, L. Yu, M.A. Valentin, A. Jeromin, H. Zetterberg, O. Hansson, N. Mattsson-Carlgren, D. Graham, K. Blennow, J. H. Kramer, L.T. Grinberg, W.W. Seeley, H. Rosen, B.F. Boeve, B.L. Miller, C. E. Teunissen, G.D. Rabinovici, J.C. Rojas, J.L. Dage, A.L. Boxer, Plasma phosphorylated tau 217 and phosphorylated tau 181 as biomarkers in Alzheimer's disease and frontotemporal lobar degeneration: a retrospective diagnostic performance study, Lancet Neurol. 20 (9) (2021) 739–752.

[32] H.M. Snyder, M.C. Carrillo, F. Grodstein, K. Henriksen, A. Jeromin, S. Lovestone, M.M. Mielke, S. O'Bryant, M. Sarasa, M. Sjögren, H. Soares, J. Teeling, E. Trushina, M. Ward, T. West, L.J. Bain, D.W. Shineman, M. Weiner, H.M. Fillit, Developing novel blood-based biomarkers for Alzheimer's disease, Alzheimer's. Dement.: J. Alzheimer's Assoc. 10 (1) (2014) 109–114.

[33] V. Mantzavinos, A. Alexiou, Biomarkers for Alzheimer's disease diagnosis, Curr. Alzheimer Res. 14 (11) (2017) 1149–1154.

[34] P.G. Raje, S.R. Gurav, M.R. Waikar, A.S. Rasal, J.-Y. Chang, R.G. Sonkawade, The review of different dimensionalities based pristine metal organic frameworks for supercapacitor application, J. Energy Storage 56 (2022), 105700.

[35] S.A. Sawant, A.V. Patil, M.R. Waikar, A.S. Rasal, S.D. Dhas, A.V. Moholkar, R. S. Vhatkar, R.G. Sonkawade, Advances in chemical and biomass-derived graphene/graphene-like nanomaterials for supercapacitors, J. Energy Storage 51 (2022), 104445.

[36] F. Hakimian, H. Ghourchian, A.S. Hashemi, M.R. Arastoo, M. Behnam Rad, Ultrasensitive optical biosensor for detection of miRNA-155 using positively charged Au nanoparticles, Sci. Rep. 8 (1) (2018), 2943.

[37] E. Scarpa, V.M. Mastronardi, F. Guido, L. Algieri, A. Qualtieri, R. Fiammengo, F. Rizzi, M. De Vittorio, Wearable piezoelectric mass sensor based on pH sensitive hydrogels for sweat pH monitoring, Sci. Rep. 10 (1) (2020), 10854.

[38] M. Wang, Y. Yang, J. Min, Y. Song, J. Tu, D. Mukasa, C. Ye, C. Xu, N. Heflin, J. S. McCune, T.K. Hsiai, Z. Li, W. Gao, A wearable electrochemical biosensor for the monitoring of metabolites and nutrients, Nat. Biomed. Eng. 6 (11) (2022) 1225–1235.

[39] S.M. Borisov, O.S. Wolfbeis, Optical biosensors, Chem. Rev. 108 (2) (2008) 423–461.

[40] V. Vongsouthi, J.H. Whitfield, P. Unichenko, J.A. Mitchell, B. Breithausen, O. Khersonsky, L. Kremers, H. Janovjak, H. Monai, H. Hirase, S.J. Fleishman, C. Henneberger, C.J. Jackson, A rationally and computationally designed fluorescent biosensor for d-Serine, ACS Sens. 6 (11) (2021) 4193–4205.

[41] W. Nawrot, K. Drzozga, S. Baluta, J. Cabaj, K. Malecha, A fluorescent biosensors for detection vital body fluids' agents, Sens. (Basel, Switz.) 18 (8) (2018).

[42] S., d Manzeli, D. Ovchinnikov, O.V.Yazyev pasquier, A. Kis, Nat. Rev. Mater. 2 (2017), 17033.

[43] B. Chamlagain, S.S. Withanage, A.C. Johnston, S.I. Khondaker, Scalable lateral heterojunction by chemical doping of 2D TMD thin films, Sci. Rep. 10 (1) (2020), 12970.

[44] X. Luo, X. Lin, F. Gao, Y. Zhao, X. Li, L. Zhan, Z. Qiu, J. Wang, C. Chen, L. Meng, Recent progress in perovskite solar cells: from device to commercialization, Sci. China Chem. 65 (12) (2022) 2369–2416.

[45] L. Kong, X. Zhou, G. Shi, Y. Yu, Molybdenum disulfide nanosheets-based fluorescent "off-to-on" probe for targeted monitoring and inhibition of β-amyloid oligomers, Analyst 145 (19) (2020) 6369–6377.

[46] A. Huang, L. Zhang, W. Li, Z. Ma, S. Shuo, T. Yao, Controlled fluorescence quenching by antibody-conjugated graphene oxide to measure tau protein, R. Soc. Open Sci. 5 (4) (2018), 171808.

[47] H.I. Kim, D. Yim, S.J. Jeon, T.W. Kang, I.J. Hwang, S. Lee, J.K. Yang, J.M. Ju, Y. So, J.H. Kim, Modulation of oligonucleotide-binding dynamics on WS(2) nanosheet interfaces for detection of Alzheimer's disease biomarkers, Biosens. Bioelectron. 165 (2020), 112401.

[48] O'sullivan, C.; Vaughan, R.; Guilbault, G., Piezoelectric immunosensors-theory and applications. 1999.

[49] P. Martinkova, A. Kostelnik, T. Valek, M. Pohanka, Main streams in the construction of biosensors and their applications, Int. J. Electrochem. Sci. 12 (8) (2017) 7386–7403.

[50] Z. Tavakolian-Ardakani, O. Hosu, C. Cristea, M. Mazloum-Ardakani, G. Marrazza, Latest trends in electrochemical sensors for neurotransmitters: a review, Sens. (Basel, Switz.) 19 (9) (2019).

[51] K. Rajpoot, Recent advances and applications of biosensors in novel technology, Biosens. J. 6 (2) (2017) 1–12.

[52] B. Shui, D. Tao, A. Florea, J. Cheng, Q. Zhao, Y. Gu, W. Li, N. Jaffrezic-Renault, Y. Mei, Z. Guo, Biosensors for Alzheimer's disease biomarker detection: a review, Biochimie 147 (2018) 13–24.

[53] E. Bakker, E. Pretsch, Potentiometric sensors for trace-level analysis, Trends Anal. Chem.: TRAC 24 (3) (2005) 199–207.

[54] G. Getachew, A. Wibrianto, A.S. Rasal, W.B. Dirersa, J.-Y. Chang, Metal halide perovskite nanocrystals for biomedical engineering: recent advances, challenges, and future perspectives, Coord. Chem. Rev. 482 (2023), 215073.

[55] E. Cesewski, B.N. Johnson, Electrochemical biosensors for pathogen detection, Biosens. Bioelectron. 159 (2020), 112214.

[56] M. Azimzadeh, N. Nasirizadeh, M. Rahaie, H. Naderi-Manesh, Early detection of Alzheimer's disease using a biosensor based on electrochemically-reduced graphene oxide and gold nanowires for the quantification of serum microRNA-137, RSC Adv. 7 (88) (2017) 55709–55719.

[57] M.N. Sonuç Karaboga, M.K. Sezgintürk, Analysis of Tau-441 protein in clinical samples using rGO/AuNP nanocomposite-supported disposable impedimetric neuro-biosensing platform: towards Alzheimer's disease detection, Talanta 219 (2020) 121257.

[58] L. Zhu, Z. Zhao, P. Cheng, Z. He, Z. Cheng, J. Peng, H. Wang, C. Wang, Y. Yang, Z. Hu, Antibody-mimetic peptoid nanosheet for label-free serum-based diagnosis of Alzheimer's disease, Adv. Mater. (Deerfield Beach, Fla.) 29 (30) (2017).

[59] C. Toyos-Rodríguez, F.J. García-Alonso, A. de la Escosura-Muñiz, Electrochemical biosensors based on nanomaterials for early detection of Alzheimer's disease, Sens. (Basel, Switz.) 20 (17) (2020).

[60] M. Zhou, Y. Zhai, S. Dong, Electrochemical sensing and biosensing platform based on chemically reduced graphene oxide, Anal. Chem. 81 (14) (2009) 5603–5613.

[61] K. Balasubramanian, K. Kern, 25th anniversary article: label-free electrical biodetection using carbon nanostructures, Adv. Mater. (Deerfield Beach, Fla.) 26 (8) (2014) 1154–1175.

[62] J. Sethi, M. Van Bulck, A. Suhail, M. Safarzadeh, A. Perez-Castillo, G. Pan, A label-free biosensor based on graphene and reduced graphene oxide dual-layer for electrochemical determination of beta-amyloid biomarkers, Mikrochim. Acta 187 (5) (2020), 288.

[63] D.L. Brody, H. Jiang, N. Wildburger, T.J. Esparza, Non-canonical soluble amyloid-beta aggregates and plaque buffering: controversies and future directions for target discovery in Alzheimer's disease, Alzheimer's. Res. Ther. 1 (2017) 62.

[64] A. Hector, J. Brouillette, Hyperactivity induced by soluble Amyloid-β oligomers in the early stages of Alzheimer's disease, Front. Mol. Neurosci. 13 (2020), 600084.

[65] L. Sun, Y. Zhong, J. Gui, X. Wang, X. Zhuang, J. Weng, A hydrogel biosensor for high selective and sensitive detection of amyloid-beta oligomers, Int. J. Nanomed. 13 (2018) 843–856.

[66] H.J. Qiu, Y. Guan, P. Luo, Y. Wang, Recent advance in fabricating monolithic 3D porous graphene and their applications in biosensing and biofuel cells, Biosens. Bioelectron. 89 (Pt 1) (2017) 85–95.

[67] E. Ferrari, Gold nanoparticle-based plasmonic biosensors, Biosensors 13 (3) (2023).

[68] G. Congur, E. Eksin, A. Erdem, Impedimetric detection of miRNA-34a using graphene oxide modified chemically activated graphite electrodes, Sens. Actuators A: Phys. 279 (2018) 493–500.

[69] J.W. Shin, K.J. Kim, J. Yoon, J. Jo, W.A. El-Said, J.W. Choi, Silver nanoparticle modified electrode covered by graphene oxide for the enhanced electrochemical detection of dopamine, Sens. (Basel, Switz.) 17 (12) (2017).

[70] S.S. Choo, E.S. Kang, I. Song, D. Lee, J.W. Choi, T.H. Kim, Electrochemical detection of dopamine using 3D porous graphene oxide/gold nanoparticle composites, Sens. (Basel, Switz.) 17 (4) (2017).

[71] C. Wang, J. Li, K. Shi, Q. Wang, X. Zhao, Z. Xiong, X. Zou, Y. Wang, Graphene coated by polydopamine/multi-walled carbon nanotubes modified electrode for highly selective detection of dopamine and uric acid in the presence of ascorbic acid, J. Electroanal. Chem. 770 (2016) 56–61.

[72] D. Deletioglu, E. Hasdemir, A. O Solak, Simultaneous determination of dopamine and uric acid in the presence of ascorbic acid at the indole-3-carboxaldehyde modified glassy carbon electrode, Curr. Anal. Chem. 6 (3) (2010) 203–208.

[73] D.-J. Park, J.-H. Choi, W.-J. Lee, S.H. Um, B.-K. Oh, Selective electrochemical detection of dopamine using reduced graphene oxide sheets-gold nanoparticles modified electrode, J. Nanosci. Nanotechnol. 17 (11) (2017) 8012–8018.

[74] E.J. Lee, J.-H. Choi, S.H. Um, B.-K. Oh, Electrochemical sensor for selective detection of norepinephrine using graphene sheets-gold nanoparticle complex modified electrode, Korean J. Chem. Eng. 34 (2017) 1129–1132.

[75] L. Wang, Y. Zhang, C. Cheng, X. Liu, H. Jiang, X. Wang, Highly sensitive electrochemical biosensor for evaluation of oxidative stress based on the nanointerface of graphene nanocomposites blended with gold, Fe3O4, and platinum nanoparticles, ACS Appl. Mater. Interfaces 7 (33) (2015) 18441–18449.

[76] D. Jeong, J. Kim, M.S. Chae, W. Lee, S.H. Yang, Y. Kim, S.M. Kim, J.S. Lee, J. H. Lee, J. Choi, D.S. Yoon, K.S. Hwang, Multifunctionalized reduced graphene oxide biosensors for simultaneous monitoring of structural changes in Amyloid-β 40, Sens. (Basel, Switz.) 18 (6) (2018).

[77] S. Nangare, P. Patil, Chitosan mediated layer-by-layer assembly based graphene oxide decorated surface plasmon resonance biosensor for highly sensitive detection of β-amyloid, Int. J. Biol. Macromol. 214 (2022) 568–582.

[78] S. Nangare, P. Patil, Poly(allylamine) coated layer-by-layer assembly decorated 2D carbon backbone for highly sensitive and selective detection of Tau-441 using surface plasmon resonance biosensor, Anal. Chim. Acta 1271 (2023), 341474.

[79] A.M.M. Murillo, M.F. Laguna, L.G. Valle, L. Tramarin, Y. Ramirez, Á. Lavín, B. Santamaría, M. Holgado, A new optical interferometric biosensing system enhanced with nanoparticles for Alzheimer's disease in serum, Biosensors 13 (7) (2023) 707.

[80] X. Zuo, H. Dai, H. Zhang, J. Liu, S. Ma, X. Chen, A peptide-WS(2) nanosheet based biosensing platform for determination of β-secretase and screening of its inhibitors, Analyst 143 (19) (2018) 4585–4591.

[81] A. Battigelli, J.H. Kim, D.C. Dehigaspitiya, C. Proulx, E.J. Robertson, D.J. Murray, B. Rad, K. Kirshenbaum, R.N. Zuckermann, Glycosylated peptoid nanosheets as a multivalent scaffold for protein recognition, ACS Nano 12 (3) (2018) 2455–2465.

[82] J. Sun, R.N. Zuckermann, Peptoid polymers: a highly designable bioinspired material, ACS Nano 7 (6) (2013) 4715–4732.

[83] K. Kirshenbaum, R.N. Zuckermann, Peptoids in wonderland, Biopolymers 110 (4) (2019), e23279.

[84] C.L. Chen, R.N. Zuckermann, J.J. DeYoreo, Surface-directed assembly of sequence-defined synthetic polymers into networks of hexagonally patterned nanoribbons with controlled functionalities, ACS Nano 10 (5) (2016) 5314–5320.

[85] X. Ma, S. Zhang, F. Jiao, C.J. Newcomb, Y. Zhang, A. Prakash, Z. Liao, M.D. Baer, C.J. Mundy, J. Pfaendtner, A. Noy, C.L. Chen, J.J. De Yoreo, Tuning crystallization pathways through sequence engineering of biomimetic polymers, Nat. Mater. 16 (7) (2017) 767–774.

[86] M. Chhowalla, H.S. Shin, G. Eda, L.J. Li, K.P. Loh, H. Zhang, The chemistry of two-dimensional layered transition metal dichalcogenide nanosheets, Nat. Chem. 5 (4) (2013) 263–275.

[87] S. Manzeli, D. Ovchinnikov, D. Pasquier, O.V. Yazyev, A. Kis, 2D transition metal dichalcogenides, Nat. Rev. Mater. 2 (8) (2017) 1–15.

[88] Q.H. Wang, K. Kalantar-Zadeh, A. Kis, J.N. Coleman, M.S. Strano, Electronics and optoelectronics of two-dimensional transition metal dichalcogenides, Nat. Nanotechnol. 7 (11) (2012) 699–712.

[89] K.F. Mak, C. Lee, J. Hone, J. Shan, T.F. Heinz, Atomically thin MoS₂: a new direct-gap semiconductor, Phys. Rev. Lett. 105 (13) (2010), 136805.

[90] W. Zhao, Z. Ghorannevis, L. Chu, M. Toh, C. Kloc, P.H. Tan, G. Eda, Evolution of electronic structure in atomically thin sheets of WS2 and WSe2, ACS nano 7 (1) (2013) 791–797.

[91] X. Huang, Z. Zeng, H. Zhang, Metal dichalcogenide nanosheets: preparation, properties and applications, Chem. Soc. Rev. 42 (5) (2013) 1934–1946.

[92] O. Lopez-Sanchez, D. Lembke, M. Kayci, A. Radenovic, A. Kis, Ultrasensitive photodetectors based on monolayer MoS2, Nat. Nanotechnol. 8 (7) (2013) 497–501.

[93] F. Raza, D. Yim, J.H. Park, H.I. Kim, S.J. Jeon, J.H. Kim, Structuring Pd nanoparticles on 2H-WS(2) nanosheets induces excellent photocatalytic activity for cross-coupling reactions under visible light, J. Am. Chem. Soc. 139 (41) (2017) 14767–14774.

[94] J. Xu, J. Zhang, W. Zhang, C.S. Lee, Interlayer nanoarchitectonics of two-dimensional transition-metal dichalcogenides nanosheets for energy storage and conversion applications, Adv. Energy Mater. 7 (23) (2017), 1700571.

[95] H. Hu, A. Zavabeti, H. Quan, W. Zhu, H. Wei, D. Chen, J.Z. Ou, Recent advances in two-dimensional transition metal dichalcogenides for biological sensing, Biosens. Bioelectron. 142 (2019), 111573.

[96] X.L. Hu, L. Chu, X. Dong, G.R. Chen, T. Tang, D. Chen, X.P. He, H. Tian, Multivalent glycosheets for double light–driven therapy of multidrug-resistant bacteria on wounds, Adv. Funct. Mater. 29 (14) (2019), 1806986.

[97] K. Kalantar-zadeh, J.Z. Ou, T. Daeneke, M.S. Strano, M. Pumera, S.L. Gras, Two-dimensional transition metal dichalcogenides in biosystems, Adv. Funct. Mater. 25 (32) (2015) 5086–5099.

[98] T.W. Kang, J. Han, S. Lee, I.J. Hwang, S.J. Jeon, J.M. Ju, M.J. Kim, J.K. Yang, B. Jun, C.H. Lee, S.U. Lee, J.H. Kim, 2D transition metal dichalcogenides with glucan multivalency for antibody-free pathogen recognition, Nat. Commun. 9 (1) (2018), 2549.

[99] J. Chen, R. Zhang, C. Tao, X. Huang, Z. Chen, X. Li, J. Zhou, Q. Zeng, B. Zhao, M. Yuan, M. Ma, Z. Wu, CuS-NiS(2) nanomaterials for MRI guided phototherapy of gastric carcinoma via triggering mitochondria-mediated apoptosis and MLKL/CAPG-mediated necroptosis, Nanotoxicology 14 (6) (2020) 774–787.

[100] J. Ge, Y.-H. Du, J.-J. Chen, L. Zhang, D.-M. Bai, D.-Y. Ji, Y.-L. Hu, Z.-H. Li, Highly sensitive fluorescence detection of mercury (II) ions based on WS2 nanosheets and T7 exonuclease assisted cyclic enzymatic amplification, *Sens.* Actuators B: Chem. 249 (2017) 189–194.

[101] X. Zuo, H. Zhang, Q. Zhu, W. Wang, J. Feng, X. Chen, A dual-color fluorescent biosensing platform based on WS2 nanosheet for detection of Hg(2+) and Ag(.), Biosens. Bioelectron. 85 (2016) 464–470.

[102] K.-J. Huang, Y.-J. Liu, H.-B. Wang, T. Gan, Y.-M. Liu, L.-L. Wang, Signal amplification for electrochemical DNA biosensor based on two-dimensional graphene analogue tungsten sulfide–graphene composites and gold nanoparticles, *Sens.* Actuators B: Chem. 191 (2014) 828–836.

[103] E. Rahmanian, C.C. Mayorga-Martinez, R. Malekfar, J. Luxa, Z. Sofer, M. Pumera, 1T-phase tungsten chalcogenides (WS2, WSe2, WTe2) decorated with TiO2 nanoplatelets with enhanced electron transfer activity for biosensing applications, ACS Appl. Nano Mater. 1 (12) (2018) 7006–7015.

[104] C. Sui, T. Wang, Y. Zhou, H. Yin, X. Meng, S. Zhang, G.I.N. Waterhouse, Q. Xu, Y. Zhuge, S. Ai, Photoelectrochemical biosensor for hydroxymethylated DNA detection and T4-β-glucosyltransferase activity assay based on WS(2) nanosheets and carbon dots, Biosens. Bioelectron. 127 (2019) 38–44.

[105] I.M. Khan, S. Niazi, Y. Yu, A. Mohsin, B.S. Mushtaq, M.W. Iqbal, A. Rehman, W. Akhtar, Z. Wang, Aptamer induced multicolored AuNCs-WS(2) "Turn on" FRET nano platform for dual-color simultaneous detection of AflatoxinB(1) and zearalenone, Anal. Chem. 91 (21) (2019) 14085–14092.

[106] Y. Yuan, R. Li, Z. Liu, Establishing water-soluble layered WS₂ nanosheet as a platform for biosensing, Anal. Chem. 86 (7) (2014) 3610–3615.

[107] Q. Xi, D.M. Zhou, Y.Y. Kan, J. Ge, Z.K. Wu, R.Q. Yu, J.H. Jiang, Highly sensitive and selective strategy for microRNA detection based on WS2 nanosheet mediated fluorescence quenching and duplex-specific nuclease signal amplification, Anal. Chem. 86 (3) (2014) 1361–1365.

[108] J. Zhao, X. Jin, M. Vdovenko, L. Zhang, I.Y. Sakharov, S. Zhao, A WS2 nanosheet chemiluminescence resonance energy transfer platform for sensing biomolecules, Chem. Commun. (Camb., Engl.) 51 (55) (2015) 11092–11095.

[109] Y. Qin, Y. Ma, X. Jin, L. Zhang, G. Ye, S. Zhao, A sensitive fluorescence turn-on assay of bleomycin and nuclease using WS2 nanosheet as an effective sensing platform, Anal. Chim. Acta 866 (2015) 84–89.

[110] J. Zhao, Y. Ma, R. Kong, L. Zhang, W. Yang, S. Zhao, Tungsten disulfide nanosheet and exonuclease III co-assisted amplification strategy for highly sensitive fluorescence polarization detection of DNA glycosylase activity, Anal. Chim. Acta 887 (2015) 216–223.

[111] M. Naguib, O. Mashtalir, J. Carle, V. Presser, J. Lu, L. Hultman, Y. Gogotsi, M. W. Barsoum, Two-dimensional transition metal carbides, ACS Nano 6 (2) (2012) 1322–1331.

[112] N. Özcan, H. Medetalibeyoglu, O. Akyıldırım, N. Atar, M.L. Yola, Electrochemical detection of amyloid-β protein by delaminated titanium carbide MXene/multi-walled carbon nanotubes composite with molecularly imprinted polymer, Mater. Today Commun. 23 (2020), 101097.

[113] Y. Chen, Z. Chen, Y. Sun, J. Lei, G. Wei, Mechanistic insights into the inhibition and size effects of graphene oxide nanosheets on the aggregation of an amyloid-β peptide fragment, Nanoscale 10 (19) (2018) 8989–8997.

[114] F. Chiti, C.M. Dobson, Protein misfolding, amyloid formation, and human disease: a summary of progress over the last decade, Annu. Rev. Biochem. 86 (2017) 27–68.

[115] C.A. Ross, M.A. Poirier, Protein aggregation and neurodegenerative disease, Nat. Med. 10 (*Suppl*) (2004) S10–S17.

[116] R. Nelson, M.R. Sawaya, M. Balbirnie, A. Madsen, C. Riekel, R. Grothe, D. Eisenberg, Structure of the cross-beta spine of amyloid-like fibrils, Nature 435 (7043) (2005) 773–778.

[117] D.M. Walsh, I. Klyubin, J.V. Fadeeva, W.K. Cullen, R. Anwyl, M.S. Wolfe, M. J. Rowan, D.J. Selkoe, Naturally secreted oligomers of amyloid beta protein potently inhibit hippocampal long-term potentiation in vivo, Nature 416 (6880) (2002) 535–539.

[118] S. Lesné, M.T. Koh, L. Kotilinek, R. Kayed, C.G. Glabe, A. Yang, M. Gallagher, K. H. Ashe, A specific amyloid-beta protein assembly in the brain impairs memory, Nature 440 (7082) (2006) 352–357.

[119] M. Zhang, S. Mao, Y. Yu, C.X. Wang, Y.L. Yang, C. Wang, Nanomaterials for reducing amyloid cytotoxicity, Adv. Mater. (Deerfield Beach, Fla.) 25 (28) (2013) 3780–3801.

[120] W.-H. Xi, G.-H. Wei, Amyloid-β peptide aggregation and the influence of carbon nanoparticles, Chin. Phys. B 25 (1) (2015), 018704.

[121] Y.H. Liao, Y.J. Chang, Y. Yoshiike, Y.C. Chang, Y.R. Chen, Negatively charged gold nanoparticles inhibit Alzheimer's amyloid-β fibrillization, induce fibril dissociation, and mitigate neurotoxicity, Small (Weinh. der Bergstr., Ger.) 8 (23) (2012) 3631–3639.

[122] Q. Ma, G. Wei, X. Yang, Influence of Au nanoparticles on the aggregation of amyloid-β-(25-35) peptides, Nanoscale 5 (21) (2013) 10397–10403.

[123] C. Cabaleiro-Lago, F. Quinlan-Pluck, I. Lynch, S. Lindman, A.M. Minogue, E. Thulin, D.M. Walsh, K.A. Dawson, S. Linse, Inhibition of amyloid beta protein fibrillation by polymeric nanoparticles, J. Am. Chem. Soc. 130 (46) (2008) 15437–15443.

[124] Q. Wang, X. Yu, K. Patal, R. Hu, S. Chuang, G. Zhang, J. Zheng, Tanshinones inhibit amyloid aggregation by amyloid-β peptide, disaggregate amyloid fibrils, and protect cultured cells, ACS Chem. Neurosci. 4 (6) (2013) 1004–1015.

[125] B. Bohrmann, K. Baumann, J. Benz, F. Gerber, W. Huber, F. Knoflach, J. Messer, K. Oroszlan, R. Rauchenberger, W.F. Richter, C. Rothe, M. Urban, M. Bardroff, M. Winter, C. Nordstedt, H. Loetscher, Gantenerumab: a novel human anti-Aβ antibody demonstrates sustained cerebral amyloid-β binding and elicits cell-mediated removal of human amyloid-β, J. Alzheimer'S. Dis.: JAD 28 (1) (2012) 49–69.

[126] J. Sevigny, P. Chiao, T. Bussière, P.H. Weinreb, L. Williams, M. Maier, R. Dunstan, S. Salloway, T. Chen, Y. Ling, J. O'Gorman, F. Qian, M. Arastu, M. Li, S. Chollate,

M.S. Brennan, O. Quintero-Monzon, R.H. Scannevin, H.M. Arnold, T. Engber, K. Rhodes, J. Ferrero, Y. Hang, A. Mikulskis, J. Grimm, C. Hock, R.M. Nitsch, A. Sandrock, The antibody aducanumab reduces Aβ plaques in Alzheimer's disease, Nature 537 (7618) (2016) 50–56.

[127] T. Takahashi, H. Mihara, Peptide and protein mimetics inhibiting amyloid beta-peptide aggregation, Acc. Chem. Res. 41 (10) (2008) 1309–1318.

[128] M. Mahmoudi, O. Akhavan, M. Ghavami, F. Rezaee, S.M. Ghiasi, Graphene oxide strongly inhibits amyloid beta fibrillation, Nanoscale 4 (23) (2012) 7322–7325.

[129] Z. Yang, C. Ge, J. Liu, Y. Chong, Z. Gu, C.A. Jimenez-Cruz, Z. Chai, R. Zhou, Destruction of amyloid fibrils by graphene through penetration and extraction of peptides, Nanoscale 7 (44) (2015) 18725–18737.

[130] Q. Li, L. Liu, S. Zhang, M. Xu, X. Wang, C. Wang, F. Besenbacher, M. Dong, Modulating aβ33-42 peptide assembly by graphene oxide, Chem. (Weinh. der Bergstr., Ger.) 20 (24) (2014) 7236–7240.

[131] J. Wang, Y. Cao, Q. Li, L. Liu, M. Dong, Size effect of graphene oxide on modulating amyloid peptide assembly, Chem. (Weinh. der Bergstr., Ger. 21 (27) (2015) 9632–9637.

[132] J. Wang, Z. Zhu, C. Bortolini, S.V. Hoffmann, A. Amari, H.X. Zhang, L. Liu, M. D. Dong, Dimensionality of carbon nanomaterial impacting on the modulation of amyloid peptide assembly, Nanotechnology 27 (30) (2016), 304001.

[133] Y. Liu, L.P. Xu, W. Dai, H. Dong, Y. Wen, X. Zhang, Graphene quantum dots for the inhibition of β amyloid aggregation, Nanoscale 7 (45) (2015) 19060–19065.

[134] L. Baweja, K. Balamurugan, V. Subramanian, A. Dhawan, Effect of graphene oxide on the conformational transitions of amyloid beta peptide: a molecular dynamics simulation study, J. Mol. Graph. Model. 61 (2015) 175–185.

[135] M. Li, X. Yang, J. Ren, K. Qu, X. Qu, Using graphene oxide high near-infrared absorbance for photothermal treatment of Alzheimer's disease, Adv. Mater. (Deerfield Beach, Fla.) 24 (13) (2012) 1722–1728.

[136] G. Qing, S. Zhao, Y. Xiong, Z. Lv, F. Jiang, Y. Liu, H. Chen, M. Zhang, T. Sun, Chiral effect at protein/graphene interface: a bioinspired perspective to understand amyloid formation, J. Am. Chem. Soc. 136 (30) (2014) 10736–10742.

[137] N. Zhang, X. Hu, P. Guan, K. Zeng, Y. Cheng, Adsorption mechanism of amyloid fibrils to graphene nanosheets and their structural destruction, J. Phys. Chem. C. 123 (1) (2018) 897–906.

[138] S. Xiao, D. Zhou, P. Luan, B. Gu, L. Feng, S. Fan, W. Liao, W. Fang, L. Yang, E. Tao, R. Guo, J. Liu, Graphene quantum dots conjugated neuroprotective peptide improve learning and memory capability, Biomaterials 106 (2016) 98–110.

[139] P. Nedumpully-Govindan, E.N. Gurzov, P. Chen, E.H. Pilkington, W.J. Stanley, S. A. Litwak, T.P. Davis, P.C. Ke, F. Ding, Graphene oxide inhibits hIAPP amyloid fibrillation and toxicity in insulin-producing NIT-1 cells, Phys. Chem. Chem. Phys.: PCCP 18 (1) (2016) 94–100.

[140] Q. Li, J. Froning, M. Pykal, S. Zhang, Z. Wang, M. Vondrák, P. Banáš, K. Čépe, P. Jurečka, J. Šponer, RNA nanopatterning on graphene, 2D Mater. 5 (3) (2018), 031006.

[141] M. Li, A. Zhao, K. Dong, W. Li, J. Ren, X. Qu, Chemically exfoliated WS 2 nanosheets efficiently inhibit amyloid β-peptide aggregation and can be used for photothermal treatment of Alzheimer's disease, Nano Res. 8 (2015) 3216–3227.

[142] W. Chen, J. Ouyang, X. Yi, Y. Xu, C. Niu, W. Zhang, L. Wang, J. Sheng, L. Deng, Y. N. Liu, S. Guo, Black phosphorus nanosheets as a neuroprotective nanomedicine for neurodegenerative disorder therapy, Adv. Mater. (Deerfield Beach, Fla.) 30 (3) (2018).

[143] W. Lei, T. Zhang, P. Liu, J.A. Rodriguez, G. Liu, M. Liu, Bandgap-and local field-dependent photoactivity of Ag/black phosphorus nanohybrids, ACS Catal. 6 (12) (2016) 8009–8020.

[144] W. Chen, J. Ouyang, H. Liu, M. Chen, K. Zeng, J. Sheng, Z. Liu, Y. Han, L. Wang, J. Li, L. Deng, Y.N. Liu, S. Guo, Black phosphorus nanosheet-based drug delivery system for synergistic photodynamic/photothermal/chemotherapy of cancer, Adv. Mater. (Deerfield Beach, Fla.) 29 (5) (2017).

[145] H. Kwon, S.W. Seo, T.G. Kim, E.S. Lee, P.T. Lanh, S. Yang, S. Ryu, J.W. Kim, Ultrathin and flat layer black phosphorus fabricated by reactive oxygen and water rinse, ACS Nano 10 (9) (2016) 8723–8731.

[146] Q. Zhou, Q. Chen, Y. Tong, J. Wang, Light-induced ambient degradation of few-layer black phosphorus: mechanism and protection, Angew. Chem. Int. Ed. Engl. 55 (38) (2016) 11437–11441.

[147] J. Yang, W. Liu, Y. Sun, X. Dong, LVFFARK-PEG-stabilized black phosphorus nanosheets potently inhibit amyloid-β fibrillogenesis, Langmuir: ACS J. Surf. Colloids 36 (7) (2020) 1804–1812.

[148] Y.J. Lim, W. h Zhou, G. Li, Z.W. Hu, L. Hong, X.F. Yu, Y.M. Lim, Black phosphorus nanomaterials regulate the aggregation of Amyloid-β, ChemNanoMat 5 (5) (2019) 606–611.

[149] K. AnjiReddy, S. Karpagam, Chitosan nanofilm and electrospun nanofiber for quick drug release in the treatment of Alzheimer's disease: in vitro and in vivo evaluation, Int. J. Biol. Macromol. 105 (Pt 1) (2017) 131–142.

[150] V. Saharan, A. Mehrotra, R. Khatik, P. Rawal, S.S. Sharma, A. Pal, Synthesis of chitosan based nanoparticles and their in vitro evaluation against phytopathogenic fungi, Int. J. Biol. Macromol. 62 (2013) 677–683.

[151] C. Tang, Y.X. Guan, S.J. Yao, Z.Q. Zhu, Preparation of ibuprofen-loaded chitosan films for oral mucosal drug delivery using supercritical solution impregnation, Int. J. Pharm. 473 (1-2) (2014) 434–441.

[152] M. Li, Y. Guan, Z. Chen, N. Gao, J. Ren, K. Dong, X. Qu, Platinum-coordinated graphitic carbon nitride nanosheet used for targeted inhibition of amyloid β-peptide aggregation, Nano Res. 9 (2016) 2411–2423.

[153] M. Li, Y. Guan, C. Ding, Z. Chen, J. Ren, X. Qu, An ultrathin graphitic carbon nitride nanosheet: a novel inhibitor of metal-induced amyloid aggregation associated with Alzheimer's disease, J. Mater. Chem. B 4 (23) (2016) 4072–4075.

[154] Y. Zheng, Y. Jiao, J. Chen, J. Liu, J. Liang, A. Du, W. Zhang, Z. Zhu, S.C. Smith, M. Jaroniec, G.Q. Lu, S.Z. Qiao, Nanoporous graphitic-C3N4@carbon metal-free electrocatalysts for highly efficient oxygen reduction, J. Am. Chem. Soc. 133 (50) (2011) 20116–20119.

[155] S.C. Yan, Z.S. Li, Z.G. Zou, Photodegradation performance of g-C3N4 fabricated by directly heating melamine, Langmuir: ACS J. Surf. Colloids 25 (17) (2009) 10397–10401.

[156] T. Komatsu, Attempted chemical synthesis of graphite-like carbon nitride, J. Mater. Chem. 11 (3) (2001) 799–801.

[157] Y. Zheng, L. Lin, B. Wang, X. Wang, Graphitic carbon nitride polymers toward sustainable photoredox catalysis, Angew. Chem. Int. Ed. Engl. 54 (44) (2015) 12868–12884.

[158] J. Zhang, Y. Chen, X. Wang, Two-dimensional covalent carbon nitride nanosheets: synthesis, functionalization, and applications, Energy Environ. Sci. 8 (11) (2015) 3092–3108.

[159] Y. Hou, Z. Wen, S. Cui, X. Guo, J. Chen, Constructing 2D porous graphitic C3 N4 nanosheets/nitrogen-doped graphene/layered MoS2 ternary nanojunction with enhanced photoelectrochemical activity, Adv. Mater. (Deerfield Beach, Fla.) 25 (43) (2013) 6291–6297.

[160] Y. Fang, Y. Lv, R. Che, H. Wu, X. Zhang, D. Gu, G. Zheng, D. Zhao, Two-dimensional mesoporous carbon nanosheets and their derived graphene nanosheets: synthesis and efficient lithium ion storage, J. Am. Chem. Soc. 135 (4) (2013) 1524–1530.

[161] J. Tian, Q. Liu, C. Ge, Z. Xing, A.M. Asiri, A.O. Al-Youbi, X. Sun, Ultrathin graphitic carbon nitride nanosheets: a low-cost, green, and highly efficient electrocatalyst toward the reduction of hydrogen peroxide and its glucose biosensing application, Nanoscale 5 (19) (2013) 8921–8924.

[162] Q. Wang, W. Wang, J. Lei, N. Xu, F. Gao, H. Ju, Fluorescence quenching of carbon nitride nanosheet through its interaction with DNA for versatile fluorescence sensing, Anal. Chem. 85 (24) (2013) 12182–12188.

[163] X. Zhang, X. Xie, H. Wang, J. Zhang, B. Pan, Y. Xie, Enhanced photoresponsive ultrathin graphitic-phase C3N4 nanosheets for bioimaging, J. Am. Chem. Soc. 135 (1) (2013) 18–21.

[164] J. Wang, Z. Zhang, H. Zhang, C. Li, M. Chen, L. Liu, M. Dong, Enhanced photoresponsive graphene oxide-modified g-C(3)N(4) for disassembly of Amyloid β Fibrils, ACS Appl. Mater. Interfaces 11 (1) (2019) 96–103.

[165] C. Ren, D. Li, Q. Zhou, X. Hu, Mitochondria-targeted TPP-MoS(2) with dual enzyme activity provides efficient neuroprotection through M1/M2 microglial polarization in an Alzheimer's disease model, Biomaterials 232 (2020), 119752.

[166] S. Bernard, P. Miele, Nanostructured and architectured boron nitride from boron, nitrogen and hydrogen-containing molecular and polymeric precursors, Mater. Today 17 (9) (2014) 443–450.

[167] J.H. Kim, T.V. Pham, J.H. Hwang, C.S. Kim, M.J. Kim, Boron nitride nanotubes: synthesis and applications, Nano Converg. 5 (1) (2018), 17.

[168] S.M. Sharker, M.A. Alam, M.C. Shill, G.M.S. Rahman, H.M. Reza, Functionalized hBN as targeted photothermal chemotherapy for complete eradication of cancer cells, Int. J. Pharm. 534 (1-2) (2017) 206–212.

[169] X. Chen, P. Wu, M. Rousseas, D. Okawa, Z. Gartner, A. Zettl, C.R. Bertozzi, Boron nitride nanotubes are noncytotoxic and can be functionalized for interaction with proteins and cells, J. Am. Chem. Soc. 131 (3) (2009) 890–891.

[170] N. Izyumskaya, D.O. Demchenko, S. Das, Ü. Özgür, V. Avrutin, H. Morkoç, Recent development of boron nitride towards electronic applications, Adv. Electron. Mater. 3 (5) (2017), 1600485.

[171] A. Merlo, V. Mokkapati, S. Pandit, I. Mijakovic, Boron nitride nanomaterials: biocompatibility and bio-applications, Biomater. Sci. 6 (9) (2018) 2298–2311.

[172] A. Kurz, R. Perneczky, Novel insights for the treatment of Alzheimer's disease, Prog. Neuro-Psychopharmacol. Biol. Psychiatry 35 (2) (2011) 373–379.

[173] Ö. Yıldırım, M.E. Arslan, S. Öner, I. Cacciatore, A. Di Stefano, A. Mardinoglu, H. Turkez, Boron nitride nanoparticles loaded with a boron-based hybrid as a promising drug carrier system for Alzheimer's disease treatment, Int. J. Mol. Sci. 23 (15) (2022).

[174] F. Kar, C. Hacıoğlu, Y. Göncü, İ. Söğüt, H. Şenturk, D. Burukoğlu Dönmez, G. Kanbak, N. Ay, In vivo assessment of the effect of hexagonal boron nitride nanoparticles on biochemical, histopathological, oxidant and antioxidant status, J. Clust. Sci. 32 (2021) 517–529.

[175] A. Ucar, V. Parlak, F.B. Ozgeris, A.C. Yeltekin, M.E. Arslan, G. Alak, H. Turkez, E. M. Kocaman, M. Atamanalp, Magnetic nanoparticles-induced neurotoxicity and oxidative stress in brain of rainbow trout: mitigation by ulexite through modulation of antioxidant, anti-inflammatory, and antiapoptotic activities, Sci. Total Environ. 838 (Pt 1) (2022), 155718.

[176] N. Aydin, H. Turkez, O.O. Tozlu, M.E. Arslan, M. Yavuz, E. Sonmez, O.F. Ozpolat, I. Cacciatore, A. Di Stefano, A. Mardinoglu, Ameliorative effects by hexagonal boron nitride nanoparticles against beta amyloid induced neurotoxicity, Nanomater. (Basel, Switz.) 12 (2022) 15.

[177] O. Bull, I. Bull, G. Amadi, C. Odu, Covalent organic frameworks (COFs): a review, J. Appl. Sci. Environ. Manag. 26 (1) (2022) 145–179.

[178] S. Patial, V. Soni, A. Kumar, P. Raizada, T. Ahamad, X.M. Pham, Q.V. Le, V. H. Nguyen, S. Thakur, P. Singh, Rational design, structure properties, and synthesis strategies of dual-pore covalent organic frameworks (COFs) for potent applications: a review, Environ. Res. 218 (2023), 114982.

[179] S.N.A. Bukhari, N. Ahmad, M.W. Amjad, M.A. Hussain, M.A. Elsherif, H. Ejaz, N. H. Alotaibi, Covalent organic frameworks (COFs) as multi-target multifunctional frameworks, Polymers 15 (2) (2023).

[180] R. Maleki, M. Khedri, S. Rezvantalab, F. Afsharchi, K. Musaie, S. Shafiee, M. A. Shahbazi, β-Amyloid targeting with two-dimensional covalent organic

frameworks: multi-scale in-silico dissection of nano-biointerface, Chembiochem: A Eur. J. Chem. Biol. 22 (13) (2021) 2306–2318.

[181] C. Du, W. Feng, X. Dai, J. Wang, D. Geng, X. Li, Y. Chen, J. Zhang, Cu(2+) -chelatable and ROS-scavenging MXenzyme as NIR-II-triggered blood-brain barrier-crossing nanocatalyst against Alzheimer's disease, Small (Weinh. der Bergstr., Ger.) 18 (39) (2022), e2203031.

[182] Y. Jiang, Y. Kang, J. Liu, S. Yin, Z. Huang, L. Shao, Nanomaterials alleviating redox stress in neurological diseases: mechanisms and applications, J. Nanobiotechnol. 20 (1) (2022), 265.

[183] K. Li, Q. Ji, H. Liang, Z. Hua, X. Hang, L. Zeng, H.J. Han, Biomedical application of 2D nanomaterials in neuroscience, J. Nanobiotechnol. 21 (1) (2023) 181.

[184] T.W. Kang, S.J. Jeon, H.I. Kim, J.H. Park, D. Yim, H.R. Lee, J.M. Ju, M.J. Kim, J. H. Kim, Optical detection of enzymatic activity and inhibitors on non-covalently functionalized fluorescent graphene oxide, ACS Nano 10 (5) (2016) 5346–5353.